Journal of Advanced Research 69 (2025) 279–297

Contents lists available at ScienceDirect

Journal of Advanced Research

journal homepage: www.elsevier.com/locate/jare

Original Manuscript

Exercise-Induced Reduction of IGF1R Sumoylation Attenuates Neuroinflammation in APP/PS1 Transgenic Mice

Yisheng Chen [a,1], Xiaofeng Chen [b,1], Zhiwen Luo [a,1], Xueran Kang [c,1], Yunshen Ge [a,1], Renwen Wan [a], Qian Wang [d], Zhihua Han [e], Fangqi Li [a], Zhongcheng Fan [f], Yuchun Xie [g], Beijie Qi [a], Xintao Zhang [h], Zhenwei Yang [i], John H Zhang [j,*], Danping Liu [i,*], Yuzhen Xu [k,*], Dongyan Wu [a,*], Shiyi Chen [a,*]

[a] Huashan Hospital, Fudan University, Shanghai, China
[b] Department of Orthopaedics, National Regional Medical Center, Jinjiang Municipal Hospital,Shanghai Sixth People's Hospital, Fujian, Jinjiang,China
[c] Shanghai Jiao Tong University School of Medicine, Shanghai Jiao Tong University, China
[d] Department of Central Laboratory, The Affiliated Taian City Central Hospital of Qingdao University, Taian, Shandong, China
[e] Department of Orthopedics, Shanghai General Hospital, Shanghai Jiao Tong University School of Medicine, Shanghai Jiao Tong University, Shanghai 200080, China
[f] Department of Orthopaedic Surgery, Hainan Province Clinical Medical Center, Haikou Affiliated Hospital of Central South University Xiangya School of Medicine, China
[g] Jiangsu Province Geriatric Hospital, China
[h] Department of Sports Medicine and Rehabilitation, Peking University Shenzhen Hospital Lianhua Road, Shenzhen City, Guangdong Province, China
[i] Department of Orthopaedics, First Affiliated Hospital of Jinzhou Medical University, Jinzhou, Liaoning Province, China
[j] Department of Neurosurgery, Department of Physiology and Pharmacology, Department of Neurosurgery and Anesthesiology, School of Medicine, Loma Linda University, Risley Hall, Room 219, 11041 Campus Street, Loma Linda, CA, 92354, USA
[k] Department of Rehabilitation, The Second Affiliated Hospital of Shandong First Medical University, Taian, Shandong, China

HIGHLIGHTS

- Physical activity ameliorates the symptoms of Alzheimer's Disease (AD) in APP/PS1 mice, with a notable reduction in neuroinflammatory indicators such as IL-1β, IL-6, and TNF-α.
- Desumoylation mutations of IGF1R play a pivotal role in attenuating neuroinflammation associated with AD.
- Physical activity exerts a significant influence on the nuclear translocation of SUMO1 and IGF1R.
- KPT330 effectively inhibits the formation of the IGF1R/RanBP2/SUMO1 complex, thereby bolstering cognitive functionality.
- KPT330 emerges as a promising substitute for physical exercise in therapeutic strategies targeting AD.

GRAPHICAL ABSTRACT

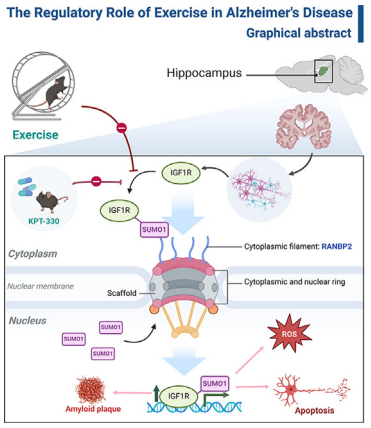

* Corresponding authors at: Department of Sports Medicine, Huashan Hospital, Fudan University, Shanghai, China. (S. Chen). Department of Sports Medicine, Huashan Hospital, Fudan University, Shanghai, China. (D. Wu). Department of Rehabilitation, The Second Affiliated Hospital of Shandong First Medical University, Taian, Shandong Province 271000, China. (Y. Xu). Department of Orthopaedics, First Affiliated Hospital of Jinzhou Medical University, Jinzhou, Liaoning Province, China. (D. Liu). Department of Neurosurgery, Department of Physiology and Pharmacology, Department of Neurosurgery and Anesthesiology, School of Medicine, Loma Linda University, Risley Hall, Room 219, 11041 Campus Street, Loma Linda, CA, 92354, USA. (J.H. Zhang).

E-mail addresses: feng5313@hotmail.com (X. Chen), johnzhang3910@yahoo.com (J.H Zhang), liudanping2009@sohu.com (D. Liu), tianyayizhe@126.com (Y. Xu), walkwinter@163.com (D. Wu), cshiyi@163.com (S. Chen).

[1] These authors contributed equally to this work.

https://doi.org/10.1016/j.jare.2024.03.025
2090-1232/

ARTICLE INFO

Article history:
Received 17 October 2023
Revised 3 February 2024
Accepted 29 March 2024
Available online 31 March 2024

Keywords:
Alzheimer's Disease
IGF1R sumoylation
Neuroinflammation
Exercise
KPT-330
SUMOylation inhibitor

ABSTRACT

Introduction: Alzheimer's Disease (AD), a progressive neurodegenerative disorder, is marked by cognitive deterioration and heightened neuroinflammation. The influence of Insulin-like Growth Factor 1 Receptor (IGF1R) and its post-translational modifications, especially sumoylation, is crucial in understanding the progression of AD and exploring novel therapeutic avenues.
Objectives: This study investigates the impact of exercise on the sumoylation of IGF1R and its role in ameliorating AD symptoms in APP/PS1 mice, with a specific focus on neuroinflammation and innovative therapeutic strategies.
Methods: APP/PS1 mice were subjected to a regimen of moderate-intensity exercise. The investigation encompassed assessments of cognitive functions, alterations in hippocampal protein expressions, neuroinflammatory markers, and the effects of exercise on IGF1R and SUMO1 nuclear translocation. Additionally, the study evaluated the efficacy of KPT-330, a nuclear export inhibitor, as an alternative to exercise.
Results: Exercise notably enhanced cognitive functions in AD mice, possibly through modulations in hippocampal proteins, including Bcl-2 and BACE1. A decrease in neuroinflammatory markers such as IL-1β, IL-6, and TNF-α was observed, indicative of reduced neuroinflammation. Exercise modulated the nuclear translocation of SUMO1 and IGF1R in the hippocampus, thereby facilitating neuronal regeneration. Mutant IGF1R (MT IGF1R), lacking SUMO1 modification sites, showed reduced SUMOylation, leading to diminished expression of pro-inflammatory cytokines and apoptosis. KPT-330 impeded the formation of the IGF1R/RanBP2/SUMO1 complex, thereby limiting IGF1R nuclear translocation, inflammation, and neuronal apoptosis, while enhancing cognitive functions and neuron proliferation.
Conclusion: Moderate-intensity exercise effectively mitigates AD symptoms in mice, primarily by diminishing neuroinflammation, through the reduction of IGF1R Sumoylation. KPT-330, as a potential alternative to physical exercise, enhances the neuroprotective role of IGF1R by inhibiting SUMOylation through targeting XPO1, presenting a promising therapeutic strategy for AD.

Introduction

Alzheimer's Disease (AD) is a prevalent neurodegenerative disorder that poses a significant public health concern worldwide [1,2]. Characterized by cognitive decline, memory loss, and distinctive behavioral changes, AD involves complex molecular pathways, including inflammation, cell apoptosis, and dysregulation of protein metabolism [3]. The multifaceted pathogenesis of AD continues to present challenges in developing effective treatments, underscoring the need for novel and comprehensive therapeutic strategies [4].

Physical exercise has emerged as a potent non-pharmacological intervention in AD management, given its myriad health benefits [5,6]. Extensive research has highlighted the cognitive-enhancing impacts of exercise on both neurologically healthy individuals and those afflicted by neurodegenerative disorders [7–10]. Exercise has been demonstrated to augment cerebral blood flow, thereby enhancing the brain's nutrient and oxygen supply, fostering the health and functional restoration of the nervous system [11,12]. Exercise also modulates neuroinflammatory responses, possibly by reducing pro-inflammatory cytokines, and interferes with the deposition of β-amyloid (Aβ) proteins, a key pathological hallmark of AD, potentially through the upregulation of Aβ clearance pathways [13,14]. Moreover, exercise exerts beneficial effects on glucose metabolism, potentially preventing metabolic conditions that may exacerbate neurodegeneration [15–18]. Recent research has unveiled that physical activity may potentially influence the IGF1R pathway, a correlation that could be associated with neurodegenerative changes [19]. This study aims to elucidate the mechanistic role of the insulin-like growth factor 1 receptor (IGF-1R) signaling pathway in AD and its potential modulation by physical exercise [20]. IGF-1R, a membrane receptor with tyrosine kinase activity, is abundantly present in the brain and significantly contributes to cellular growth, proliferation, and survival [21]. Recent findings suggest that a reduction in IGF-1R activity could be associated with AD pathogenesis, indicating that enhancing IGF-1R signaling might offer a promising approach for AD management [21]. The study of protein modification processes and their implications in neurodegenerative diseases has been a subject of intense research in recent years. One such process, SUMOylation, has been linked to the stability, activity, and subcellular location of proteins, notably the Insulin-like Growth Factor 1 Receptor (IGF-1R) [22,23].

Recent investigations suggest a potential correlation between nuclear translocation, a process involving the movement of proteins between the nucleus and the cytoplasm, and the progression of Alzheimer's Disease [24–26]. Particularly noteworthy is the role of RanBP2 and Small Ubiquitin-like Modifier 1 (SUMO1), two proteins that play an integral part in the SUMOylation of the Insulin-like Growth Factor 1 Receptor (IGF-1R) [27,28]. The proteins RanBP2 and SUMO1, known to play vital roles in IGF-1R SUMOylation, a protein modification process affecting its stability, activity, and subcellular location, will be a central part of the investigation [29,30].

The phenomenon of nuclear translocation, the transfer of proteins between the nucleus and the cytoplasm, has emerged as a focal point of interest [31]. This process, fundamental to cellular function, has been implicated in the pathogenesis of numerous diseases, including the insidious AD. The significance of this study lies in its exploration of the enigmatic relationship between nuclear translocation and the progression of AD. This study proposes that physical exercise could inhibit the nuclear translocation of IGF-1R by suppressing its SUMOylation, thereby possibly counteracting AD pathogenesis.

Moreover, XPO1 is a critical component of SUMO1 nuclear translocation. XPO1 plays a significant role in neurodegenerative diseases such as Amyotrophic Lateral Sclerosis and Frontotemporal Dementia (ALS/FTD) [32,33]. For instance, in ALS/FTD research, XPO1 inhibitors have been found to reduce cell death induced by overexpression of TAR DNA-binding protein 43 (TDP43) in cortical neurons, suggesting a neuroprotective role for XPO1 [34].In another study, overexpression of XPO1 effectively promoted the export of nuclear TDP43, whereas high cytoplasmic concentrations of TDP43 inhibited neuronal survival [32]. Additionally, XPO1 exercises its nuclear protein export function, regulating cell cycle, apoptosis, and death [35–37]. XPO1, as an exporter of over 200

known cargoes, such as p53, p21, IκB-α, and NF-κB [36].Inhibition of XPO1 may impact numerous inflammation/immune pathways associated with neurological disorders, such as Nrf2, FOXOs, and NF-κB signaling pathways [32]. This study assesses the potential of KPT-330 (an XPO1 inhibitor) as a surrogate for physical exercise, revealing the prospective utility of genetic and material therapeutics, which is particularly pivotal for individuals constrained by physical limitations or other health conditions that preclude regular exercise [38,39]. We hypothesize that KPT-330 might influence the functionality of the nuclear pore complex, including RanBP2 and SUMO1, thereby affecting IGF1R SUMOylation and potentially preventing AD.

In summary, this research aims to provide novel insights into the complex interplay between physical activity and neurodegenerative diseases, particularly AD. By unraveling this innovative mechanistic pathway, we hope to contribute to the expanding body of evidence supporting the protective effect of exercise on cognitive health. If our hypothesis is correct, it could potentially change the approach to managing AD, emphasizing the role of physical exercise and exercise substitutes like KPT-330 in maintaining cognitive health and providing a shield against the debilitating cognitive decline associated with Alzheimer's disease.

Material and methods

Animal experimental model

We utilized the APP/PS1 transgenic mouse strain (MMRRC Strain #034829-JAX, Stock No. 004462) obtained from Jackson Laboratory (B6;C3-Tg(APPswe,PSEN1dE9)85Dbo/Mmjax). These mice express chimeric mouse/human amyloid precursor protein (Mo/HuAPP695swe) and a mutated human presenilin 1 (PS1-dE9), both localized in the neurons of the central nervous system and associated with early-onset Alzheimer's disease, as indicated in previous studies [40–42]. The male APP/PS1 mice and their wild-type C57BL/6J counterparts were acquired from the Model Animal Research Center of Nanjing University, ensuring uniformity in genetic background and eliminating the impact of sex differences on Alzheimer's disease-related cognitive impairment. We selected male mice at 8 weeks of age, with an average weight of 20–26 g. All mice were housed in a specific pathogen-free (SPF) laboratory environment, maintaining a stable temperature of 22–25 °C and a 12-hour light–dark cycle, with ad libitum access to food and water. Standard polypropylene cages (290 × 180 × 160 mm) were used for housing each group of mice separately to minimize the influence of individual housing on social behavior. Mice in the exercise group had free access to a running wheel with a diameter of 12 cm. Our experimental procedures were in strict compliance with the guidelines of the Institutional Animal Care and Use Committee and had received approval from the local ethical committee. The study was conducted under double-blind conditions, adhering to the Guide for Care. We made every effort to reduce animal distress.

Ethics statement

All investigations implicating the utilization of animals were executed in strict accordance with ethical policies and sanctioned procedures, endorsed by the Ethical Committee of Huashan Hospital. All experimental protocols involving animals rigorously conformed to the ARRIVE guidelines and meticulously adhered to prevailing regulations and directives relevant to animal research. Every animal study has received the explicit approval of the Institutional Review Board of Huashan Hospital (2023-HSYY-136JZS).

Exercise protocol and reagents

The exercise protocol was designed based on the principles of physiological adaptation and overload related to exercise, and in reference to the study by Fernando et al [43,44]. on mouse exercise intensity. The regimen was designed to gradually increase exercise intensity over a 90-day period [45]. As previously described [46], the exercise regimen consisted of two stages.Initially, all exercise groups underwent 7 days of adaptive training. This "pre-intervention period" was designed to habituate the mice to the exercise regimen. The exercise speed and duration were set at 5 m/min for 15 min on days 1–2, 8 m/min for 15 min on days 3–4, and 12 m/min for 15 min on days 5–7. Following a 2-day rest period, a 3-month formal training phase commenced, with 30 min of exercise scheduled daily, five days a week. The training sessions were conducted from 18:00 to 20:00. The WTE and ADE groups underwent treadmill exercise, with the high-intensity exercise group (HEX) gradually increasing speed from 12 m/min to 15 m/min. According to the study by Schefer et al. [46], this regimen represented a load intensity of 60 % to 73 % of the maximum oxygen uptake (VO_2 max), indicative of moderate-intensity aerobic exercise. The specific exercise regimen was as follows: the exercise groups followed the same exercise regimen, starting with 5 min of exercise at 5 m/min and 8 m/min. Then, for the low-intensity exercise group, the speed was increased to 15 m/min for 15 min, or for the high-intensity exercise group, the speed was increased to 15 m/min for 30 min. Finally, the exercise ended with 5 min at 5 m/min. The control groups, WT-Con and AD-Con, were placed on a stationary treadmill. After each training session, the mice were returned to their home cages. KPT-330 (also known as selinexor, a selective inhibitor of exportin 1 (XPO-1)), was procured from InvivoChem (CAS No. 1393477–72-9, Guangzhou, China). KPT-330 was administered orally at a dose of 10 mg/kg. During the treatment, the mice allocated to the KPT-330 treatment group received an oral dose of 10 mg/kg twice weekly (on Mondays and Thursdays).

Morris water Maze test

The Morris Water Maze (MWM) test, a widely recognized method for evaluating spatial learning and memory, was conducted in a controlled environment to assess the cognitive functions of mice. The apparatus for this experiment was situated in a room with regulated lighting and consisted of a circular pool with a diameter of 120 cm, in line with standard requirements for adult mice water maze experiments. This pool was divided into four equal quadrants, each marked with distinctive proximal cues: triangle, circle, square, and star, to aid in spatial orientation. The pool's water was maintained at a temperature of 22 ± 2 °C and made opaque with non-toxic milk to conceal a dark cylindrical platform. This platform, submerged 1 cm below the water surface, served as the target for the mice to locate. The experiment spanned over six days, beginning with a 5-day training regimen followed by a spatial exploration test on the 6th day. During the training phase, mice were subjected to four trials per day, with each trial allowing a maximum duration of 60 s for the mice to find the hidden platform. Successful trials were defined by the mouse's ability to locate and remain on the platform for at least 10 s. Mice were started from different locations around the pool in each trial to prevent the memorization of a single path. Following each trial, mice were dried, given a 15-minute rest period, and then returned to their cages. The escape latency, or the time taken to locate the platform, was meticulously recorded for each trial. On the 6th day, the platform was removed for the spatial exploration test, allowing mice to swim freely for 60 s [47]. The performance indicators during this phase included the time spent in the target quadrant and the num-

ber of crossings over the platform's former location, with a crossing defined as over 40 % of the mouse's body entering the area. This specific criterion for crossing was clearly stated in the revised methods section of our manuscript. Throughout the behavioral experiment, the treatment of mice continued up until euthanasia. The collected data from the MWM test were utilized to quantitatively evaluate the spatial memory capacities of the mice. Statistical analysis methods were applied to the gathered data to discern significant differences in spatial learning and memory among the treated groups compared to controls, ensuring a robust evaluation of the cognitive effects of the interventions.

Tissue collection and processing

Following the completion of the final Morris Water Maze (MWM) test, mice were euthanized within 24 h to facilitate tissue collection and analysis. Euthanasia was conducted using an intraperitoneal injection of 1 % sodium pentobarbital at a dosage of 60 mg/kg body weight, a procedure selected for its efficiency and minimal stress to the animals, with the compound sourced from MilliporeSigma. Transcardial perfusion with 0.9 % saline was then performed using a perfusion pump. The brain was carefully extracted, divided into two hemispheres, with one hemisphere fixed overnight at 4 °C in 4 % paraformaldehyde, dehydrated in increasing concentrations of ethanol, embedded in paraffin, and sectioned into 5 μm-thick sagittal slices using a sliding microtome (SM2000R; Leica, Solms, Germany). Consecutive slices containing the hippocampus and cerebral cortex were placed on gelatin-coated slides for further staining experiments. The other hemisphere was immediately frozen in liquid nitrogen and stored at –80 °C for Western blot or enzyme-linked immunosorbent assay (ELISA) analysis.

Histological staining procedures

Histological analyses were performed using Hematoxylin and Eosin (H&E) staining for tissue structure, Nissl staining with Cresyl violet (Sigma-Aldrich, cat. no. C5042) for neuronal loss or degeneration, silver staining for neurofibrillary tangles, and BrdU (5-Bromo-2′-deoxyuridine) staining following the protocol from the BrdU Cell Proliferation Kit (Invitrogen, cat. no. 2750) to assess cell proliferation. The Click-iT® EdU (5-ethynyl-2′-deoxyuridine) Imaging Kits (Invitrogen, cat. no. C10339) were used to visualize newly synthesized DNA, marking cells in the S phase of the cell cycle.

In Situ cell death detection

Apoptotic neurons were assessed using the In Situ Cell Death Detection Kit (TMR red, Roche) for TdT-mediated dUTP Nick-End Labeling (TUNEL) staining. Briefly, cells were fixed in 4 % paraformaldehyde in PBS (pH 7.4) for 1 h at 4 °C, washed with PBS, and then permeabilized with a solution of 0.1 % Triton X-100 and 0.1 % sodium citrate for 2 min at 4 °C. Cells were then incubated in TUNEL reaction mixture for 1 h at 37 °C in the dark. Hoechst 33,342 was used for nuclear staining.

Detection of Reactive oxygen Species and apoptosis

Reactive Oxygen Species (ROS) were detected by staining cells with DHE (Dihydroethidium, Invitrogen, cat. no. D11347), which interacts with superoxide anions to produce red fluorescence.

Immunofluorescence staining

The capsule samples, as described above, were sectioned into thin slices. The sections were then dewaxed and rehydrated with a gradient of xylene/alcohol and PBS, and antigen retrieval was performed by placing them in EDTA antigen retrieval buffer (Servicebio, Cat: G1206, Wuhan, China) (medium heat for 8 min, interval of 8 min, medium and low heat for 7 min). The sections were then washed with PBS (pH 7.4) for 3 x 5 min. Any water surrounding the capsule was cleaned, and a circle was drawn on each tissue with a fluorescence pen. The capsule sections were then blocked in 5 % BSA and 0.5 % Triton-X-100 (Solarbio, Beijing, China) for 1 h, followed by overnight incubation at 4 °C with primary antibodies. The following day, all sections were washed three times, and after washing with PBS, the corresponding secondary antibodies were added and the sections were incubated at room temperature for 50 min. After washing with PBS, CY3-TSA (Servicebio, Cat: G1223, Wuhan, China) or FITC-TSA (Servicebio, Cat: G1222, Wuhan, China) was added, and the sections were washed on a decolorizing shaker (this step was repeated for the secondary antibody, but hydrogen peroxide sealing was avoided). DAPI staining solution (Servicebio, Cat: G1012, Wuhan, China) was added and the sections were incubated in the dark at room temperature for 10 min. For cell immunofluorescence staining, cells were fixed with 4 % paraformaldehyde for 10 min, permeabilized with 0.5 % Triton-X-100 in PBS for 10 min, and blocked with 5 % BSA for 60 min. The cells were then incubated with primary antibodies overnight at 4 °C, followed by incubation with the corresponding secondary antibodies at room temperature for 1 h. DAPI was used for counterstaining the cell nuclei. Finally, images were captured using an immunofluorescence microscope. Utilizing the image analysis software, ImageJ (contributed by Wayne Rasband and associates from the National Institutes of Health, USA), we conducted an in-depth analysis of fluorescent images. For all specimens, consistent exposure settings were maintained. To represent the relative expression levels of the target protein, we calculated the ratio of the fluorescence intensity of the target protein to that of DAPI. Every measurement was standardized under predefined threshold and parameters, ensuring analytical uniformity.

Cell cultivation and treatment

BV2 microglial cells and PC12 cells were procured from the American Type Culture Collection (ATCC, USA). The BV2 cells were cultivated in RPMI 1640 medium (Gibco, Catalog No. 11875093, USA) supplemented with 10 % fetal bovine serum (FBS, Gibco, Catalog No. 10500064, USA), 100 U/ml penicillin, and 100 μg/ml streptomycin (Sigma). The cells were maintained at 37℃ in a humidified atmosphere containing 5 % CO_2. PC12 cells were cultivated in RPMI 1640 medium supplemented with 5 % FBS and 10 % heat-inactivated horse serum (Gibco, Catalog No. 26050070, USA), 100 U/ml penicillin, and 100 μg/ml streptomycin. To differentiate PC12 cells into neuron-like cells, the culture medium was supplemented with 50 ng/ml nerve growth factor (NGF, Sigma, Catalog No. N1408, USA) and the cells were incubated for 7 days under the same conditions. The Aβ25-35 peptide (Sigma, Catalog No. A4559, USA) was reconstituted in deionized water to a concentration of 100 mM and stored at −80℃ until further use. During the experiment, cells were exposed to a culture medium containing specific concentrations of aggregated Aβ25-35 for 12 h to establish a cellular model of amyloid deposition.

Cytoplasmic and nuclear protein Extraction

Cytoplasmic and nuclear proteins were extracted using a Cytoplasmic & Nuclear Protein Extraction Kit (Beyotime, Wuhan, China) according to the manufacturer's instructions. The extracted cytoplasmic and nuclear proteins were then used for immunoblotting analysis.

Cell cultivation and transfection

In accordance with preliminary research, overexpression vectors containing the IGF1R gene and shRNA were synthesized [23,48]. Transfection was conducted following the manufacturer's instructions using Lipofectamine 3000 (Invitrogen, Carlsbad, CA, USA). In essence, shRNA IGF1R was employed to silence IGF1R. Post-transfection, spanning 24–48 h, the efficacy of IGF1R silencing was validated. Subsequently, the IGF1R overexpression vector (HA-IGF1R) and the IGF1R mutant (K1025R) vector (HA-deltaIGF1R) were separately transfected into BV2 and PC12 cells where IGF1R had already been silenced. Following a 24-hour period post-transfection, pharmacological treatment, biochemical analysis, or immunocytochemical experiments were conducted.

Quantitative Real-Time polymerase chain reaction (qRT-PCR)

The total RNA was isolated from both cellular samples and homogenized mouse brain tissue utilizing the TRIzol reagent (Invitrogen, USA). The High-Capacity cDNA Reverse Transcription Kit (Applied Biosystems) was employed to transcribe the RNA into complementary DNA (cDNA). The PCR amplification was performed according to the thermo cycler and primer parameters. The PCR steps included a denaturation step at 94 °C for 1 min, primer annealing at 55 °C for 2 min, and extension at 72 °C. Following the PCR amplification, the amplified DNA was evaluated by agarose gel electrophoresis followed by ethidium bromide staining. The housekeeping gene β-actin or GAPDH served as an internal control for the normalization of gene expression data. The relative expression of the target genes was computed using the $2^{-\Delta\Delta Ct}$ method. The analysis was conducted in triplicate to ensure precision, and the results were presented as the fold-change relative to the control group.

BCA protein concentration determination

Initially, a standard curve sample of different concentrations was prepared using a 2 μg/μl BSA standard for subsequent protein sample concentration determination. Subsequently, 10 μl of standard protein of different concentrations was added to five selected wells in a 96-well plate, and 2 μl of the protein to be tested and 8 μl of triple-distilled water were added to the remaining wells. Each well was supplemented with 200 μl of prepared BCA color reagent (Reagent A: Reagent B 50:1) and incubated at 37℃ for 20–30 min. The OD value was measured under an excitation light of 562 nm, and the relative protein concentration of the sample was finally calculated.

Cell Lysis, protein Extraction, and Co-Immunoprecipitation(CO-IP)

The culture medium was meticulously removed from the petri dishes and the cells were washed twice with precooled PBS solution. Subsequently, cells were lysed in a buffer containing Triton-X-100, 20 mM N-ethylmaleimide (NEM), protease, and phosphatase inhibitors on ice for two hours. After harvesting with a cell scraper and centrifugation at 13,000 rpm for 15 min at 4 °C, the supernatant was transferred to fresh tubes. HA-agarose beads were then prepared in precooled Triton-X-100 lysis buffer, washed, and centrifuged twice at 6,000 rpm for 1 min at 4 °C. The washed beads were incubated with the protein supernatant on a shaker at 4 °C for three hours, centrifuged, and the supernatant discarded. The beads were washed twice with Triton-X-100 lysis buffer, centrifuged, and the supernatant discarded. Finally, the lysis buffer was removed, 60 μl of 2 × loading buffer was added, and the mixture was boiled in a 95 °C metal bath for 10 min before storage at −80 °C for further analysis.

Detection of inflammatory markers by ELISA

Hippocampal tissue samples were homogenized in Tris-buffered saline containing protease inhibitors and 1 % Triton X-100. Subsequently, the samples were centrifuged at 20,000 × g for an hour, and the supernatant was collected for ELISA analysis. The concentrations of Interleukin-1β (IL-1β), Interleukin-6 (IL-6), and Tumor Necrosis Factor α (TNF-α) were quantified using the corresponding ELISA kits (Excell Biotech Corporation, Shanghai, China; Cat# EM001-96, EM004-96, EM008-96) in accordance with the manufacturer's guidelines. The absorbance at 450 nm for each well was measured by a microplate reader (Biotek Instruments, Winooski, USA), and the concentrations were determined using a standard curve prepared from standardized proteins. Similarly, the contents of BACE1, SAPPα, and SAPPβ were also determined via ELISA. The ELISA kits used were ml037908, ml127899, and ml057880 (all from Mlbio, Shanghai, China).

Cell viability Assessment

Cell viability was assessed using the Cell Counting Kit-8 (CCK-8, Sigma, USA). Prior to the assay, cells were passaged to ensure a controlled proliferation state, with the passage number kept below 20 to avoid phenotypic drift. Subsequently, cells were seeded into a 96-well plate at an appropriate density and allowed to adhere for 24 h before treatment. Post-treatment, 10 μl of CCK-8 solution was added to each well and incubated at 37 °C for a time period as per the manufacturer's instructions. Absorbance of the converted dye was measured at 450 nm using a microplate reader. The measurements were used to calculate the percentage of viable cells, with the untreated cells serving as controls for 100 % viability.

Western blotting

We executed Western blotting in accordance with previously delineated methodologies. Initially, we extracted proteins from hippocampal tissue using RIPA lysis buffer and determined the total protein concentration using a BCA Protein Assay Kit (Sangon, Shanghai, China). Subsequently, we performed the following steps: loading, electrophoresis, membrane transfer, blocking, and incubation with primary antibodies overnight and secondary antibodies for two hours. Specifically, for Western blot analysis, we subjected protein samples (20 μg) to electrophoresis on a 10 % SDS-PAGE gel, followed by transfer to a PVDF membrane using Tris-glycine buffer. We blocked using 5 % non-fat milk. We incubated with primary antibodies overnight in TBST at 4 degrees Celsius. GAPDH (Abcam, ab181602, 1:10,000) was employed as an internal control. We incubated the membrane with HRP-conjugated secondary antibodies and detected signals using an enhanced chemiluminescence (ECL) WB detection reagent. The integrated density values (IDV) of protein bands were quantified using ImageJ software.

Flow cytometry

Apoptosis in PC12 and BV2 cells was evaluated using flow cytometry. After 24 h of incubation, cells were collected by cen-

trifugation at 2000 rpm for 5 min. After washing twice with pre-cooled phosphate-buffered saline (PBS, pH 7.4), cells were suspended in binding buffer and stained with Annexin V-FITC and propidium iodide (PI) for 5 to 15 min at room temperature. Finally, these cells were analyzed by a flow cytometer (Becton Dickinson, Laguna Hills, USA).

Statistical analysis

All experimental results are presented as the mean ± standard deviation (SD)(Supplementary Table 1), and each experiment was independently conducted at least three or six times to ensure the reliability of the data. Data analysis was performed using GraphPad Prism 8.0.1 software, beginning with a normality test and a test for homogeneity of variances for each dataset. Based on these preliminary tests, appropriate statistical methods were employed: an independent sample *t*-test for data conforming to normal distribution with equal variances; Welch's *t*-test for data with normal distribution but unequal variances; and the non-parametric Mann-Whitney *U* test for data not following a normal distribution. In the case of multiple group comparisons, depending on the distribution and variance of the data, either Analysis of Variance (ANOVA) or Kruskal-Wallis H test was used, coupled with Bonferroni correction to control the false positive rate. Detailed statistical results, including the F value, degrees of freedom, and p-values for the ANOVA (Supplementary Table 1). A P-value of less than 0.05 was considered significant.

Results

Exercise modulates neurodegenerative biomarkers and neuroinflammation in APP/PS1 transgenic mice

In our investigation into the effects of exercise on Alzheimer's disease phenotype, we employed a well-established murine model using 8-week-old APP/PS1 mice, distributed across six experimental groups. Initial and subsequent body weight measurements demonstrated no significant differences between groups (Supplementary Fig. 1A & B), suggesting that the exercise regimen did not affect overall growth or health status adversely. Over a 90-day period, mice subjected to voluntary exercise showed no discernible differences in escape latency or average speed during the training phase (Supplementary Fig. 1C, D, E, and F), indicating that exercise did not influence these particular aspects of physical performance. Notably, however, the AD-HEx group displayed a remarkable improvement in cognitive function. This was evidenced by increased platform crossings and the percentage of time spent in the target quadrant during the retention phase (Fig. 1C & D), as well as extended path length (Fig. 1E), which collectively pointed to enhanced memory retention and spatial learning capabilities (Supplementary Fig. 1G). Trajectory plots further substantiated these findings, revealing a more focused navigational memory in the AD-HEx group (Fig. 1F & Supplementary Fig. 1H). Molecular analyses through Western Blot of hippocampal tissue underscored the cognitive observations. There was a significant upregulation of PSD-95 and synaptophysin proteins, coupled with a downregulation of BACE1, APP, and BAX in the AD-HEx and AD-LEx groups compared to the AD-Con group (Fig. 1G). These protein trends suggest that exercise may be influential in ameliorating apoptotic processes and reducing amyloid-beta production. Our ELISA assays provided further insights into the anti-inflammatory effects of exercise. There was a pronounced decrease in the neuroinflammatory markers IL-1β, IL-6, and TNF-α in both the AD-HEx and AD-LEx groups when juxtaposed with the AD-Con group (Fig. 1H & Supplementary Fig. 1H). This reduction in pro-inflammatory cytokines suggests a potential mitigating effect of exercise on neuroinflammation associated with Alzheimer's disease. Moreover, TUNEL staining of the hippocampal CA1 region unveiled a significant decline in apoptotic cell numbers in the AD-HEx group, as compared with the AD-Con group (Fig. 1I & Supplementary Fig. 1I), further corroborating the neuroprotective effect of exercise. In summary, our results strongly indicate that moderate-intensity exercise can serve as a beneficial intervention to alleviate the neurodegenerative phenotype and dampen neuroinflammation in an Alzheimer's disease mouse model.

Exercise regulates the nuclear translocation of SUMO1 and IGF1R

Our investigation centered on the influence of exercise on the nuclear translocation of proteins SUMO1 and IGF1R, alongside the assessment of several neurodegenerative biomarkers in mouse hippocampal tissues. The study incorporated mice from wild-type control (WT-Con), wild-type exercised (WT-LEx, WT-HEX), Alzheimer's disease control (AD-Con), and Alzheimer's disease exercised (AD-LEx, AD-HEX) groups. Western blot analysis revealed a significant modulation in the localization of SUMO1 and IGF1R post-exercise, with an enhanced nuclear presence of SUMO1 and a reduced nuclear localization of IGF1R in the exercised groups, especially in AD-HEx mice (Fig. 2A). Conversely, in the cytoplasm, SUMO1 levels decreased while IGF1R levels increased, suggesting an exercise-induced translocation of these proteins. Real-time PCR analysis confirmed that these changes were not attributed to transcriptional variations, as no significant differences were observed between the exercise and control groups (Fig. 2B & Supplementary Fig. 2A). The distribution of SUMO1 and IGF1R within the hippocampal cells, visualized through immunofluorescence, corroborated the Western blot findings; exercised mice, particularly in the AD-HEX group, showed increased nuclear localization of SUMO1 and decreased nuclear localization of IGF1R (Figs. 2C-D & Supplementary Fig. 2B). We also measured the concentrations of sAPPα, sAPPβ, and BACE1 using ELISA and observed a significant reduction in sAPPβ and BACE1 in the exercised groups compared to the control group, suggesting that exercise may impede their production (Fig. 2E & Supplementary Fig. 2C). Notably, sAPPα, known for its neuroprotective effects, was upregulated in the AD-HEx group. Immunofluorescent examinations revealed a reduction in hippocampal Aβ and caspase-3 expression and an increase in BCL-2 expression post-exercise in the AD mice. This pattern was less pronounced in the WT group, indicating a potential specificity of exercise's neuroprotective effects in the context of Alzheimer's disease (Fig. 2F & Supplementary Fig. 2D). Lastly, we evaluated neuronal regeneration using the BrdU staining technique. The results indicated that exercise enhanced neuronal regeneration in brain tissues, as evidenced by the increased BrdU-positive cells, particularly in the AD-HEX group (Fig. 2G & Supplementary Fig. 2E). This suggests that moderate-intensity exercise not only affects protein localization but may also promote neurogenesis in the diseased brain. In summary, our results elucidate the potential mechanisms by which moderate-intensity exercise could ameliorate Alzheimer's disease symptoms. The exercise-induced regulation of protein translocation, coupled with the reduced production of neurodegenerative biomarkers and enhanced neuronal regeneration, underlines the neuroprotective effects of exercise on hippocampal tissues.

Sumoylation of IGF1R promotes its nuclear translocation inducing neuroinflammatory lesions and apoptosis

In our study, we stratified cells into five distinct groups to examine the effects of Aβ25-35 on cell viability and the SUMOylation of the Insulin-like Growth Factor 1 Receptor (IGF1R), a protein

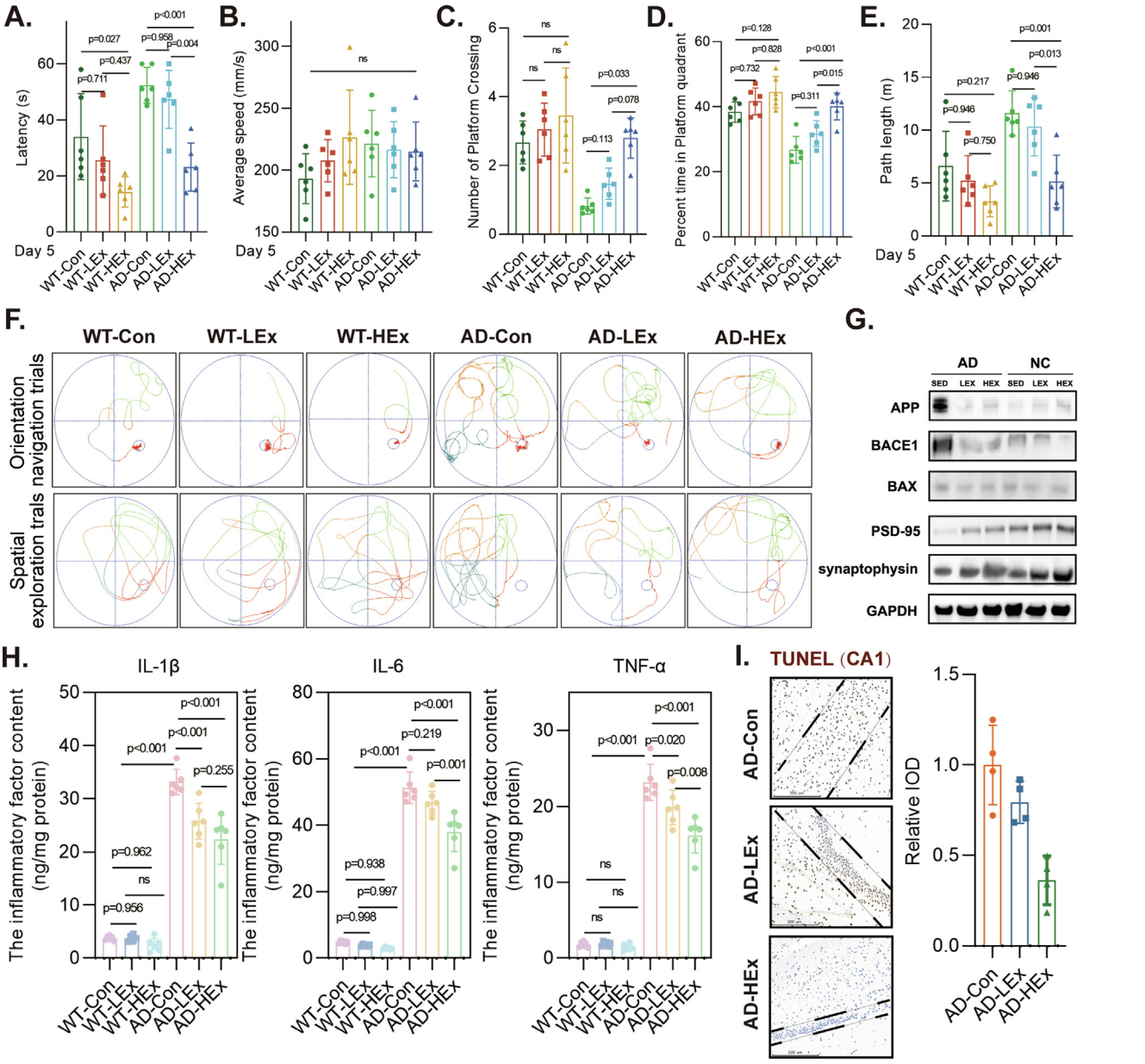

Figure 1. Impact of Exercise Intensity on Neurodegenerative Biomarkers in AD and WT Mice. (A) Evaluation of Escape Latency: The bar chart illustrates the average escape latency during the learning phase of the Morris Water Maze for various groups, with the WT-HEX and AD-HEX groups exhibiting a reduced latency by Day 5, suggesting enhanced learning. (n = 6 per group) (B) Assessment of Swimming Speed: This line graph represents the average swimming speeds during the learning phase, indicating no significant difference in swimming speed, which suggests that the observed learning improvements are independent of swimming ability. (n = 6 per group) (C) Analysis of Platform Crossings During the Retention Phase: The bar graph shows the frequency of platform crossings, with the AD-HEX group showing a higher number of crossings, indicative of better memory retention. (n = 6 per group) (D) Distribution of Time Spent in the Target Quadrant: The bar graph displays the percentage of time each group spent in the target quadrant during the retention phase, with the AD-HEX group spending more time in the target quadrant, which is consistent with improved spatial memory. (n = 6 per group) (E) Trajectory Analysis of Swimming Paths: Trajectory plots of swimming paths during the retention phase highlight the AD-HEX group's increased path length and target quadrant focus, suggesting superior navigational memory. (F) Examination of Apoptosis and AD-Associated Proteins: Western blot analysis of hippocampal proteins indicates that exercise, especially high-intensity exercise in the AD-HEX group, may contribute to a neuroprotective profile, with altered levels of apoptosis and amyloid-beta pathway proteins compared to controls. (G) Quantification of Neuroinflammatory Markers: Bar graphs showing ELISA results reveal lower levels of IL-1β, IL-6, and TNF-α in the exercise groups, especially in AD-HEX, which suggests reduced neuroinflammation due to exercise intervention. (n = 6 per group) (H) Assessment of Neuronal Apoptosis in the Hippocampal CA1 Region: TUNEL staining in the hippocampal CA1 region shows a decrease in neuronal apoptosis in the AD-HEX group, highlighting the potential neuroprotective effects of exercise. (n = 4 per group) Statistical analyses and results are detailed in Supplementary Table 1. P-values less than 0.05 were considered statistically significant. Data are represented as mean ± SD. Trends and specific values are adjusted according to provided image data.

implicated in neuroinflammatory lesions and apoptosis. Using the CCK-8 assay, we determined the survival rates of BV2 microglia and differentiated PC12 neuronal cells, identifying Aβ25-35 concentrations that optimally induced neuroinflammatory responses: 30 μm for BV2 and 50 μm for PC12 cells (Fig. 3A)(Supplementary Fig. 2F). Our experimental design involved the manipulation of IGF1R expression through wild-type and mutant constructs, with the latter lacking the SUMO1 modification site. This modification, or lack thereof, significantly influenced the cellular localization and function of IGF1R. In both BV2 and PC12 cell lines, IGF1R shRNA treatments significantly reduced IGF1R mRNA expression, whereas the expression was rescued by co-transfection with HA-tagged WT or mutant IGF1R constructs (Fig. 3B)(Supplementary Fig. 2G). Western blot analysis delineated the distribution of

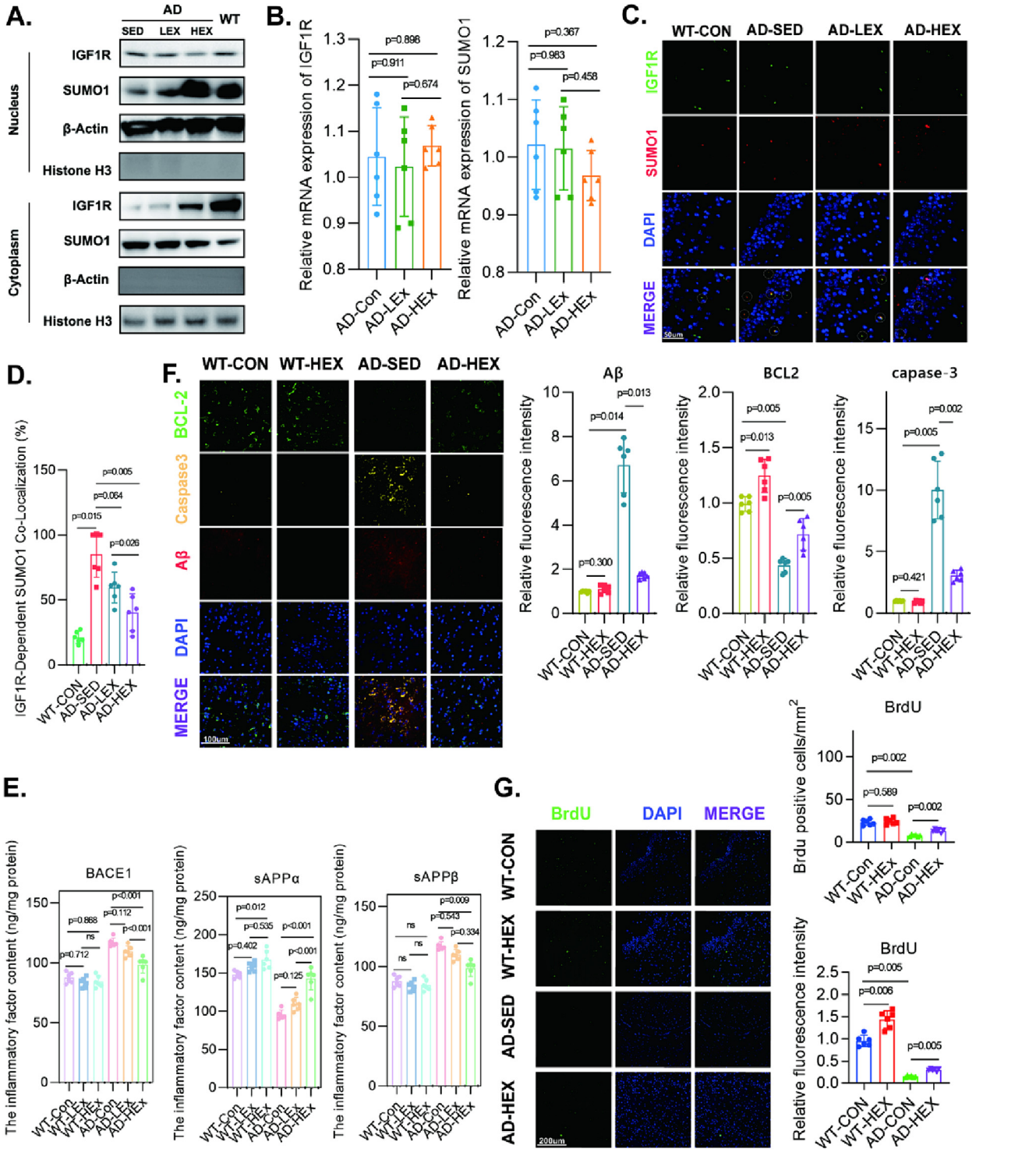

Figure 2. Impact of Exercise on SUMO1 and IGF1R Nuclear Translocation and Related Biomarkers in Mouse Hippocampal Tissues. (A) Protein Localization in Nuclear and Cytoplasmic Fractions: Western blot analysis indicates the differential localization of SUMO1 and IGF1R in nuclear and cytoplasmic compartments. An increased nuclear presence of SUMO1 and a decrease in nuclear IGF1R are apparent following exercise. Conversely, SUMO1 levels decrease and IGF1R levels increase in the cytoplasmic fraction of exercised mice, suggesting exercise-induced modulation of their localization. (B) Transcriptional Analysis of SUMO1 and IGF1R: Real-time PCR results display the transcription levels of SUMO1 and IGF1R, with no significant transcriptional changes observed between groups, indicating that exercise affects protein localization rather than transcription. (n = 6) (C) Cellular Distribution of SUMO1: Immunofluorescence staining demonstrates the spatial distribution of SUMO1 within hippocampal cells, with an increased nuclear localization in exercised mice, particularly in the AD-HEX group. (n = 6) (D) Cellular Distribution of IGF1R: Immunofluorescence staining for IGF1R shows reduced nuclear presence in exercised mice, complementing the SUMO1 distribution pattern. (n = 6) (E) Quantification of sAPPα, sAPPβ, and BACE1: ELISA results show a reduction in sAPPβ and BACE1 levels post-exercise, with an increase in sAPPα, particularly in the AD-HEx group, suggesting exercise may affect amyloid precursor protein processing. (n = 6) (F) Immunofluorescent Examination of Aβ, caspase-3, and BCL-2: Fluorescence images display the presence and localization of Aβ, caspase-3, and BCL-2 within hippocampal tissues, with a notable reduction in Aβ and caspase-3 and an increase in BCL-2 in exercised mice, indicating potential neuroprotective effects. (n = 6) (G) Assessment of Neuronal Regeneration: BrdU staining suggests enhanced neuronal regeneration in exercised mice, especially in the AD-HEX group, as shown by the increased BrdU-positive cells, indicative of active neurogenesis. (n = 6) Statistical analyses and results are detailed in Supplementary Table 1. P-values less than 0.05 were considered statistically significant. Data are represented as mean ± SD, and trends observed are in line with the proposed neuroprotective effects of exercise on hippocampal tissues.

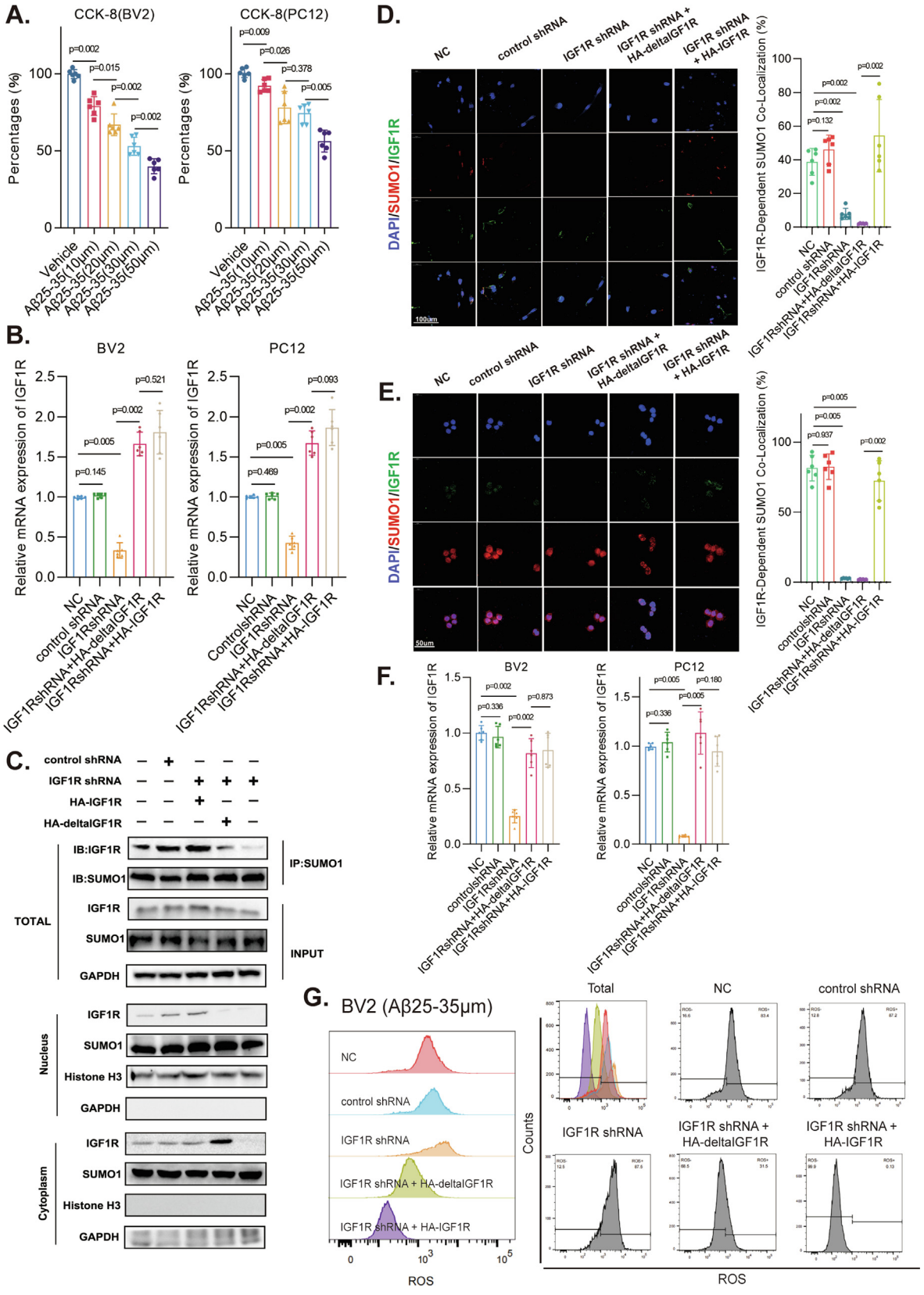
A.
CCK-8(BV2)
CCK-8(PC12)
Percentages (%)
Vehicle
Aβ25-35(10μm)
Aβ25-35(20μm)
Aβ25-35(30μm)
Aβ25-35(50μm)
B.
BV2
PC12
Relative mRNA expression of IGF1R
NC
control shRNA
IGF1RshRNA
IGF1RshRNA+HA-deltaIGF1R
IGF1RshRNA+HA-IGF1R
C.
control shRNA
IGF1R shRNA
HA-IGF1R
HA-deltaIGF1R
IB:IGF1R
IB:SUMO1
IP:SUMO1
TOTAL
IGF1R
SUMO1
GAPDH
INPUT
Nucleus
Histone H3
Cytoplasm
D.
E.
DAPI/SUMO1/IGF1R
IGF1R-Dependent SUMO1 Co-Localization (%)
F.
G.
BV2 (Aβ25-35μm)
Total
Counts
ROS

SUMO1 and IGF1R within cellular compartments. We observed that the IGF1R SUMOylation mutation (K1025R) facilitated a decrease in cytoplasmic SUMO1 and an increase in nuclear IGF1R content. This trend was absent in the WT IGF1R construct group, underscoring the role of SUMOylation in the nuclear translocation of these proteins (Fig. 3C). Immunofluorescence analyses for BV2 and PC12 cells further revealed that the mutant IGF1R (IGF1R + HA-deltaIGF1R) was predominantly localized in the cytoplasm as opposed to the nucleus, contrasting with the wild-type IGF1R, which was more nuclear (Figs. 3D-E)(Supplementary Fig. 2H). These findings were supported by quantification of fluorescence intensity, where the mutant form showed lower nuclear fluorescence intensity, confirming altered localization due to the lack of SUMOylation (Fig. 3F)(Supplementary Fig. 2I). Assessment of oxidative stress through a ROS assay corroborated these observations, indicating a reduction in apoptosis and oxidative stress in cells expressing the mutant form of IGF1R (Fig. 3G). This suggests that the SUMOylation site on IGF1R is a critical determinant of its nuclear translocation and subsequent neuroprotective or neurodestructive outcomes. In conclusion, our data support the hypothesis that SUMOylation of IGF1R is a pivotal event that promotes its nuclear translocation and contributes to the pathogenesis of neuroinflammatory lesions and apoptosis.

The neuroprotective effects of IGF1R desumoylation mutation in Alzheimer's disease cell models

In our exploration of Alzheimer's disease at the cellular level, we focused on the Insulin-like Growth Factor 1 Receptor (IGF1R) and a specific desumoylation mutation, K1025R, that inhibits SUMO1 binding. The study utilized IGF1R shRNA to downregulate the expression of IGF1R and investigated the subsequent cellular changes upon rescue with HA-tagged wild-type or mutant IGF1R constructs. Western blot analysis delineated a distinctive protein expression pattern in the IGF1RshRNA + HA-deltaIGF1R group, characterized by reduced levels of BACE1, APP, and BAX, proteins typically associated with neurodegeneration and apoptosis. Concurrently, an increase in neuroprotective protein BDNF was observed, suggesting a shift towards cell survival and neuronal protection. In stark contrast, the IGF1RshRNA + HA-IGF1R group presented an inverse expression profile, underscoring the modulatory impact of the IGF1R desumoylation mutation on these critical neuronal factors (Fig. 4A). Further investigation through EdU immunofluorescence assays revealed enhanced cell proliferation in the IGF1RshRNA + HA-deltaIGF1R group compared to the IGF1RshRNA + HA-IGF1R group, indicating that the desumoylation mutation promotes cellular proliferation (Fig. 4B)(Supplementary Fig. 2 J). ELISA analysis of inflammatory markers showed that the IGF1RshRNA + HA-IGF1R group had lower levels of TNF-α, IL-6, and IL-1β compared to the control group treated with Aβ25-35. Notably, these inflammatory cytokines were significantly reduced in the IGF1RshRNA + HA-deltaIGF1R group, highlighting the mutation's anti-inflammatory properties (Fig. 4C)(Supplementary Fig. 2 K). Flow cytometry analysis in BV2 and PC12 cell lines further supported the anti-apoptotic role of the IGF1R desumoylation mutation, showing reduced apoptosis in the IGF1RshRNA + HA-del taIGF1R group (Figs. 4D-E)(Supplementary Fig. 2L). The CCK8 assays corroborated the neuroprotective effects of the mutation, with an observed increase in cell survival rates in the IGF1RshRNA + HA-deltaIGF1R group in the face of Aβ-induced toxicity (Fig. 4F)(Supplementary Fig. 2 M). In summary, our findings suggest that the IGF1R desumoylation mutation (K1025R) provides a protective advantage in Alzheimer's disease models. This mutation seems to attenuate cellular and morphological damage, reduce inflammatory responses, and decrease apoptosis, thereby contributing to neuronal survival.

Impact of KPT-330 on IGF1R nuclear translocation and SUMO1 Colocalization: Indicators of neuroprotection

Our research into the neuroprotective effects of KPT-330 has revealed significant alterations in IGF1R nuclear translocation and SUMO1 colocalization, as well as modulations in inflammatory markers. Western blot analyses performed on nuclear and cytoplasmic fractions (Supplementary Fig. 3A) demonstrated that cells with reintroduced HA-IGF1R, when treated with KPT-330, exhibited a notable decrease in IGF1R nuclear translocation, but a significant enhancement in SUMO1 colocalization within the nucleus. This indicates that KPT-330 may impede the nuclear ingress of IGF1R and influence its colocalization with SUMO1, potentially curtailing their interaction. Quantitative assessment of caspase-3 and TNF-α expression (Supplementary Fig. 3B and C) revealed that both the KPT-330-treated group and the HA-deltaIGF1R + KPT-330 group manifested a statistically significant reduction in the expression of these markers compared to the control group (IGF1R shRNA + HA-IGF1R), suggesting potential anti-inflammatory properties of the drug. Additionally, the examination of cell apoptosis and viability through immunofluorescence (Supplementary Fig. 3D and E) provided visual and quantitative confirmation of decreased apoptosis and increased cellular vitality post-KPT-330 treatment, along with augmented SUMO1 nuclear translocation. However, these protective effects were not evident in the deltaIGF1R mutant, underscoring the necessity of an intact IGF1R for the efficacy of KPT-330. In conclusion, our data indicates that KPT-330 modulates the localization and interaction of IGF1R with SUMO1, which correlates with a reduction in inflammatory mark-

Figure 3. SUMOylation-mediated IGF1R Nuclear Translocation and its Implications on Neuroinflammation and Apoptosis. Cell Survival Rate in BV2 and PC12 Cells: The bar graph shows cell survival rates after various treatments. The optimal concentrations for inducing neuroinflammation were Aβ25-35 (30 μm) in BV2 cells and Aβ25-35 (50 μm) in PC12 cells, as demonstrated by reduced survival rates. Treatments also included control, IGF1R shRNA, and overexpression vectors HA-IGF1R and HA-deltaIGF1R. (n = 6 per group) IGF1R mRNA Expression Levels: Quantitative PCR analysis illustrates IGF1R mRNA levels in BV2 and PC12 cells. Both cell lines show increased IGF1R expression following IGF1R shRNA and HA-deltaIGF1R treatments, suggesting a regulatory effect at the transcriptional level. (n = 6 per group) (C) Protein Distribution of SUMO1 and IGF1R: Western blot panels reveal SUMO1 and IGF1R distribution in cytoplasmic and nuclear fractions. The IGF1R shRNA + HA-deltaIGF1R group exhibits a notable decrease in cytoplasmic SUMO1 and an increase in nuclear IGF1R, indicating altered protein localization through SUMOylation modification. (D) Subcellular Localization of IGF1R in BV2 Cells: Immunofluorescence images display the localization of WT IGF1R in BV2 cells, with an evident nuclear presence. (n = 6) (E) Subcellular Localization of IGF1R in PC12 Cells: Immunofluorescence images show the localization of WT and MT IGF1R in PC12 cells, where the HA-deltaIGF1R form is predominantly localized in the cytoplasm compared to the WT form, which is more nuclear. (n = 6) (F) Fluorescence Intensity Quantification of IGF1R: Bar graphs show the quantified fluorescence intensity of WT and HA-deltaIGF1R, revealing that the HA-deltaIGF1R exhibits lower nuclear fluorescence intensity, consistent with the immunofluorescence findings. (n = 6 per group) (G) ROS Assay in MT IGF1R Expressing BV2 Cells: Flow cytometry analysis displays the ROS levels in BV2 cells. Cells expressing HA-deltaIGF1R show a significant reduction in ROS, indicative of decreased oxidative stress and potential neuroprotection. (n = 6 per group) Statistical analyses, detailed in Supplementary Table 1, indicate that p-values less than 0.05 are considered statistically significant. Data are represented as mean ± SD, and trends suggest that SUMOylation modification of IGF1R might play a crucial role in neuroprotection by modulating inflammation and apoptosis pathways in response to Aβ25-35 treatment.

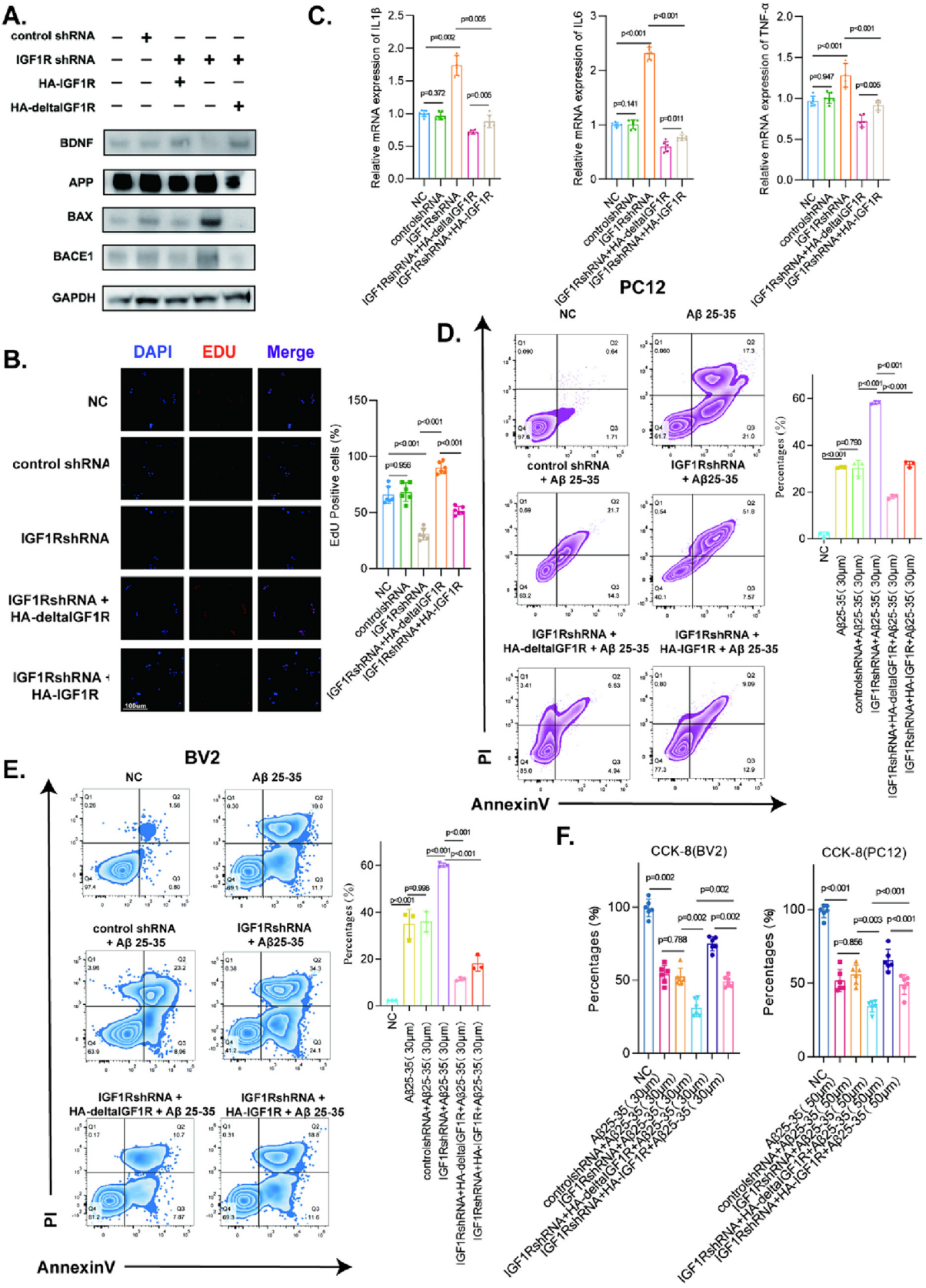
A.
control shRNA
IGF1R shRNA
HA-IGF1R
HA-deltaIGF1R
BDNF
APP
BAX
BACE1
GAPDH
B.
DAPI
EDU
Merge
NC
control shRNA
IGF1RshRNA
IGF1RshRNA + HA-deltaIGF1R
IGF1RshRNA + HA-IGF1R
100μm
EdU Positive cells (%)
C.
Relative mRNA expression of IL1β
Relative mRNA expression of IL6
Relative mRNA expression of TNF-α
PC12
D.
NC
Aβ 25-35
control shRNA + Aβ 25-35
IGF1RshRNA + Aβ25-35
IGF1RshRNA + HA-deltaIGF1R + Aβ 25-35
IGF1RshRNA + HA-IGF1R + Aβ 25-35
PI
AnnexinV
Percentages (%)
E.
BV2
F.
CCK-8(BV2)
CCK-8(PC12)
Percentages (%)

ers and apoptosis, thereby suggesting a neuroprotective mechanism.

KPT-330 as a neuroprotective agent through modulation of IGF1R/RanBP2/SUMO1 complex formation

Our study delved into the neuroprotective effects of physical exercise and the potential of KPT-330 to act as an adjunct therapy by targeting the IGF1R/RanBP2/SUMO1 protein complex. The subjects were stratified into four cohorts: a control group (AD-con) with no exercise intervention, an exercise group (AD-hex) engaging in regular physical activity, a group that ceased exercise (AD-PESG), and a final group that ceased exercise and received KPT-330 treatment (AD-PESG + KTP330). Immunoprecipitation assays indicated that regular exercise attenuated the interactions among IGF1R, RanBP2, and SUMO1 proteins when compared to the control, suggesting a suppressive effect on the formation of the IGF1R/RanBP2/SUMO1 complex (Figure 5A). Notably, this interaction was amplified upon the cessation of exercise but remained below control levels. The administration of KPT-330 post-exercise cessation further diminished the formation of this protein complex (Figure 5A). These results propose that regular exercise can disrupt the IGF1R/RanBP2/SUMO1 complex assembly, a mechanism that could underlie exercise-induced neuroprotection. The KPT-330 treatment sustained this inhibitory effect, positioning it as a viable alternative to exercise in the maintenance of neuroprotective pathways. Neurogenesis, assessed through Bromodeoxyuridine (BrdU) staining, was significantly heightened in the KPT-330 treatment group, suggesting that KPT-330 may bolster neuronal proliferation—an effect that was also observed in conjunction with physical activity (Figure 5B) (Supplementary Fig. 5A). These observations were quantitatively supported by elevated BrdU fluorescence intensity, highlighting the therapeutic potential of KPT-330 in enhancing neuronal health. ELISA analyses for inflammatory cytokines exhibited an increase in TNF-α, IL-6, and IL-1β in the AD-hex group compared to controls. Contrastingly, these markers were notably reduced in the exercise group and subsequently increased in the AD-PESG cohort, delineating the anti-inflammatory effects of the IGF1R desumoylation mutation. The beneficial effects of exercise on inflammation were preserved following KPT-330 treatment (Figure 5C)(Supplementary Fig. 5B). Further ELISA testing on hippocampal homogenate proteins associated with Alzheimer's disease revealed a decrease in BACE1 and sAPPβ levels in the exercise group relative to the control, with sAPPα levels being upregulated. The cessation of exercise reversed this pattern, suggesting that physical activity may impede the generation of β-amyloid protein. Here, KPT-330 emerged as a therapeutic agent capable of preventing the dysregulation of these proteins, akin to the effects of sustained exercise (Figure 5D)(Supplementary Fig. 5C). Lastly, apoptosis was evaluated using Caspase-3 staining, with results demonstrating a marked decrease in Caspase-3 expression in the groups treated with KPT-330, indicating a reduction in neuronal apoptosis (Figure 5E)(Supplementary Fig. 5D). The results affirm KPT-330's ability to mimic the neuroprotective benefits of physical activity by obstructing the assembly of the IGF1R/RanBP2/SUMO1 complex, thereby diminishing the nuclear translocation of IGF1R, mitigating inflammatory responses, and attenuating neuronal apoptosis.

Enhanced neuroprotection in Alzheimer's disease via inhibition of IGF1R SUMOylation by KPT-330

Our investigation reveals the profound neuroprotective properties of KPT-330, a potent antagonist of the SUMOylation pathway, in models of AD, and evaluates its efficacy relative to assorted exercise regimes. The reduction in escape latency over a span of five days was consistent (Supplementary figure 5A), signifying notable advancements in learning and memory among the cohorts treated with KPT-330. Such improvements were not ascribed to disparities in motor abilities, as evidenced by the uniform swimming velocities across the groups (Supplementary figure 5B). Cognitive evaluations conducted via the Morris Water Maze test demonstrated that AD-afflicted mice administered with KPT-330 showcased significantly enhanced memory retention and spatial navigational skills. The analysis of path lengths further corroborated that KPT-330 treatment markedly improved navigational efficiency, with treated mice locating the platform more swiftly than their control counterparts (Supplementary figure 5C). These enhancements were substantiated by a marked increase in platform crossings (Fig. 6A)(Supplementary figure 5D) and a prolonged occupancy in the target quadrant (Fig. 6B)(Supplementary figure 5E), indicative of superior cognitive performance. Molecular analyses, encompassing Western blot and immunofluorescence studies, unveiled that KPT-330 administration resulted in the diminution of pro-apoptotic proteins such as caspase-3, Bax, and APP suggesting a strategic modulation of apoptotic pathways via IGF1R desumoylation (Fig. 6D). ELISA assays lent support to these findings, revealing a decrease in BACE1 and sAPPβ levels, with a concurrent elevation in sAPPα within the hippocampal extracts of the treated groups (Fig. 6E)(Supplementary figure 5F). Furthermore, immunofluores-

Figure 4. The Protective Effect of IGF1R Desumoylation Mutation (K1025R) Against Neuronal Damage in Alzheimer's Disease. (A) Apoptosis-Related Protein Expressions Analyzed via Western Blot: The Western blot panels display protein expression levels related to apoptosis and Alzheimer's disease pathology. The IGF1RshRNA + HA-deltaIGF1R treatment group shows decreased expression of BACE1, APP, and BAX, indicating reduced cell death signaling, and increased expression of neuroprotective proteins Bcl-2 and BDNF, compared to control and HA-IGF1R groups. This suggests that the desumoylation mutation of IGF1R may confer resistance to Alzheimer's disease pathology. (n = 6 per group) (B) Fluorescence Intensity Quantification of EDU: The bar chart quantifies EDU incorporation as a measure of cell proliferation. The IGF1RshRNA + HA-deltaIGF1R group exhibited significantly increased EDU fluorescence, indicating enhanced cell survival and proliferation compared to the control shRNA group. (n = 6 per group) (C) Inflammatory Marker Levels via ELISA: The bar chart illustrates the levels of pro-inflammatory cytokines TNF-α, IL-6, and IL-1β. The IGF1RshRNA + HA-deltaIGF1R group showed a reduction in these cytokines, with the most significant decrease seen in the IGF1R + HA-deltaIGF1R group, highlighting the anti-inflammatory effects of the IGF1R desumoylation mutation. (n = 6 per group) (D) & (E) Flow Cytometry Assessment of Neuronal Apoptosis in PC12 and BV2 Cells: Scatter plots and histograms from flow cytometry analysis demonstrate the proportions of apoptotic cells. The IGF1R desumoylation mutation (K1025R) groups (IGF1RshRNA + HA-deltaIGF1R and IGF1R + HA-deltaIGF1R) exhibit reduced apoptosis, as indicated by lower Annexin V/PI staining, compared to the control groups, implying enhanced neuronal cell survival. (n = 6 per group) (F) Neuronal Survival Rates Using CCK8 Assays: The bar chart displays the cell survival rates as determined by CCK8 assays. The IGF1RshRNA + HA-deltaIGF1R group shows improved survival rates, suggesting a neuroprotective effect of the IGF1R desumoylation mutation against Aβ-induced toxicity. (n = 6 per group) Overall, the trends across the assays indicate that the IGF1R desumoylation mutation (K1025R) is associated with reduced neuronal apoptosis and inflammation, and increased cell survival, highlighting its potential as a therapeutic intervention for Alzheimer's disease. Statistical significance is denoted by p-values < 0.05, and all data are represented as mean ± SD, with detailed statistical analyses presented in Supplementary Table 1.

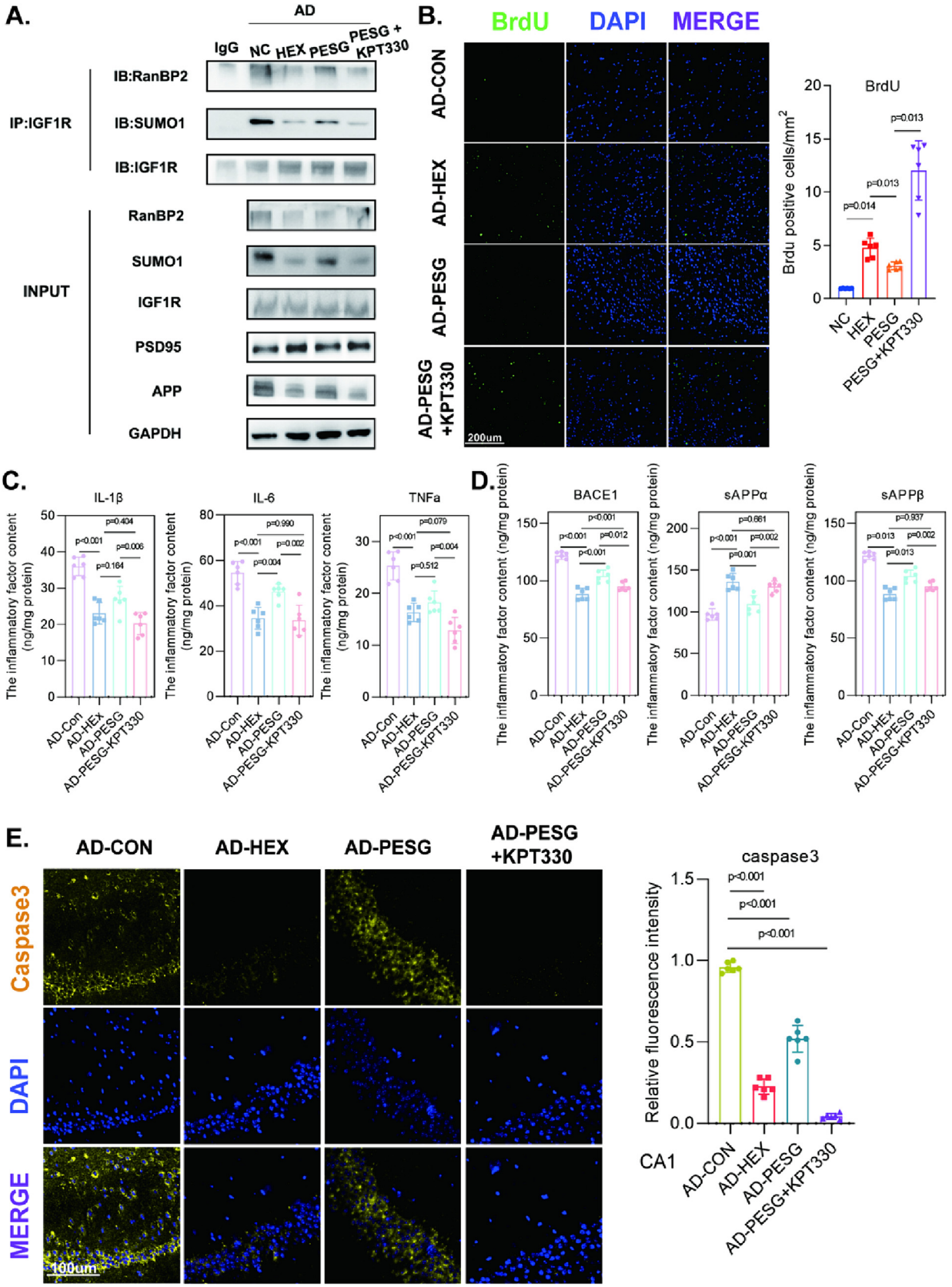
A.
AD
IgG
NC
HEX
PESG
PESG + KPT330
IP:IGF1R
IB:RanBP2
IB:SUMO1
IB:IGF1R
INPUT
RanBP2
SUMO1
IGF1R
PSD95
APP
GAPDH
B.
BrdU
DAPI
MERGE
AD-CON
AD-HEX
AD-PESG
AD-PESG +KPT330
200um
BrdU
Brdu positive cells/mm2
p=0.014
p=0.013
p=0.013
NC
HEX
PESG
PESG+KPT330
C.
IL-1β
IL-6
TNFa
The inflammatory factor content (ng/mg protein)
AD-Con
AD-HEx
AD-PESG
AD-PESG-KPT330
D.
BACE1
sAPPα
sAPPβ
E.
AD-CON
AD-HEX
AD-PESG
AD-PESG +KPT330
Caspase3
DAPI
MERGE
100um
caspase3
Relative fluorescence intensity
CA1
AD-CON
AD-HEX
AD-PESG
AD-PESG+KPT330

cence analysis displayed a notable reduction in the nuclear translocation of IGF1R in mice treated with KPT-330 (Fig. 6F)(Supplementary figure 5G), denoting the drug's inhibitory impact on the nuclear migration of IGF1R, a pivotal element in the progression of AD. Subsequent analyses of Aβ, caspase-3, and BCL-2 expression in the hippocampus post-treatment indicated a decrease in Aβ and caspase-3 levels with a simultaneous increase in BCL-2, further endorsing the neuroprotective prowess of KPT-330 (Fig. 6G)(Supplementary figure 5H). Immunofluorescence imaging has demonstrated that physical activity and KPT-330 exert an inhibitory effect on the nuclear translocation of the IGF1R within the hepatic and pulmonary tissues. Specifically, the nuclear localization of IGF1R is markedly diminished in the treated groups (AD-HEX, AD-Con + KPT330, and AD-HEX + KPT330) in comparison to the control group (AD-Con), as evidenced by the merged images. Under the treatment conditions, there is a reduced colocalization of IGF1R (green) and DAPI (blue) staining (Supplementary Figure 6A and B). This pattern aligns with the hypothesized mechanism where KPT-330, along with exercise-induced molecular adaptations, contribute to the regulation of IGF1R nuclear translocation. These results illuminate KPT-330′s crucial role in amplifying neuroprotection against Alzheimer's Disease by inhibiting the IGF1R SUMOylation process, highlighting its potential as an efficacious therapeutic approach against AD.

Discussion

Our study significantly expands our understanding of the beneficial effects of physical exercise on AD by revealing a potentially novel molecular mechanism underlying these effects. Extensive research has corroborated the salutary influence of physical activity on overall brain health, encompassing cognitive enhancement, improved neural plasticity, and diminished neuroinflammation [49,50]. Exploring the molecular complexities, our focus shifted to the Insulin-like Growth Factor 1 Receptor (IGF1R), RanBP2, and SUMO1 proteins, pivotal in various cellular processes. Our research posits a significant interaction among these proteins in relation to the progression of AD. Mirroring findings from prior studies [51–53], physical activity appears to inhibit the assembly of the IGF1R-RanBP2-SUMO1 complex, a discovery of particular significance in the realm of AD. By obstructing this complex's formation, physical exercise could confer protection against the neuronal demise and inflammation characteristic of AD.

Previous research has unveiled the potential efficacy of antioxidative stress therapies in forestalling neurodegenerative diseases linked to cognitive impairment [54,55]. Contrary to the existing body of literature, our investigation noted a pronounced diminution in the neuroinflammatory markers IL-1β, IL-6, and TNF-α in AD model mice following moderate-intensity exercise, corroborating prior studies that underscored the cognitive advantages conferred by physical activity in the context of AD [56–58]. Our study delved into the putative mechanisms of neuroprotection afforded by moderate-intensity exercise, particularly through the mitigation of cerebral inflammatory responses. Our data indicate that regular, moderate-intensity exercise significantly reduced levels of inflammatory cytokines within the hippocampal and cortical regions of AD model mice. These regions are critical for cognitive function, notably in learning and memory processes, and are among the first to be compromised in AD. Moreover, our research observed enhancements in various cognitive assessments in the exercised mice, suggesting that physical activity exerts effects not solely at the molecular level but also in behavioral domains, thereby serving a neuroprotective function. This aligns with findings that exercise bolsters the integrity of the blood–brain barrier, improves cerebrovascular function, and elevates levels of neural trophic factors within the brain. These outcomes reinforce the role of moderate-intensity exercise as a non-pharmacological intervention in neuroprotection strategies, particularly in the early intervention of AD.

Maintaining cellular metabolic homeostasis necessitates the spatiotemporal coordination of numerous critical metabolic proteins and enzymes' activities [59,60], primarily achieved through protein translocation to specific subcellular compartments and post-translational modifications [61,62]. In the context of AD, mounting evidence suggests that dysregulation of cellular processes, including aberrant intracellular protein localization, contributes to the pathology of the disease [63]. Chromosome region maintenance 1 (exportin 1, CRM1), also known as XPO1, plays a crucial role in nucleocytoplasmic transport, acting as the primary receptor for protein exportation from the nucleus [64,65]. Dysregulation of XPO1 is implicated in various aspects of AD pathology, particularly metabolic anomalies and neuroinflammation [66]. Prior research has identified XPO1 as a significant nucleocytoplasmic shuttling protein [67]. Intriguingly, SUMOylation, mediated by SUMO1 modification of IGF1R, facilitates its nuclear translocation [23,67,68]. Furthermore, SUMO1 emerges as a multifunctional architect in post-translational modification, steering various cellular navigations, including nucleocytoplasmic transport. A complex encompassing RanBP2/RanGAP1*SUMO1/Ubc9 aligns with XPO1 in promoting the nucleus-dependent functions of SUMO proteins, indicating a potential synergistic interaction or regulatory coordination between XPO1 and SUMO1 during nuclear translocation [69]. Evidence reveals that sumoylation aids the XPO1-mediated nuclear export of certain proteins [70]. For instance, SUMOylation of p53 enhances its nuclear translocation by facilitating its release from XPO1, wherein SUMO1-regulated translocation is interwoven into the fabric mediated by XPO1 [71]. The desumoylation modification of XPO1 alters its structural conformation, inhibiting its enzymatic activity and catalyzing its nuclear relocalization. We also explored the potential of KPT-330, a Selective Inhibitor of Nuclear Export (SINE) compound, as an alternative to physical exercise. Previous research has demonstrated that KPT-330 exerts

Figure 5. The Impact of KPT-330 on IGF1R Nuclear Translocation, SUMO1 Interaction, and Neuroprotective Outcomes in Alzheimer's Disease Models. (A) IGF1R Nuclear Translocation and SUMO1 Interaction: Western blot analysis shows the impact of KPT-330 treatment on IGF1R and SUMO1 protein levels in the nuclear and cytoplasmic fractions of AD model cells. An increase in nuclear IGF1R and a decrease in SUMO1 levels were observed in the presence of KPT-330, suggesting enhanced IGF1R nuclear translocation and SUMO1 dissociation. (B) Neurogenesis Assessed by BrdU Incorporation: Fluorescence microscopy images and quantitative analysis of BrdU incorporation show increased neurogenesis in AD model groups treated with KPT-330, as indicated by higher BrdU fluorescence intensity, implying enhanced cell proliferation in these groups. (n = 6 per group) (C) Inflammatory Response Evaluation by ELISA: Quantitative ELISA results for the inflammatory cytokines IL-1β, IL-6, and TNFα show a reduction in these markers in AD model cells treated with KPT-330, indicating a possible anti-inflammatory effect of the treatment. (n = 6 per group) (D) Alzheimer's Disease Marker Analysis: ELISA results demonstrate a decrease in Alzheimer's disease-related markers BACE1, sAPPα, and sAPPβ in AD model cells treated with KPT-330, highlighting the potential therapeutic effect of KPT-330 in reducing AD pathology. (n = 6 per group) (E) Apoptosis Assessment Using Caspase-3 Staining: Immunofluorescence images and quantitative analysis reveal a reduction in Caspase-3 expression in AD model groups treated with KPT-330, indicative of a decrease in apoptotic cell death. (n = 6 per group) Statistical significance is denoted by p-values < 0.05, and all data are represented as mean ± SD. Detailed statistical analyses are available in Supplementary Table 1.

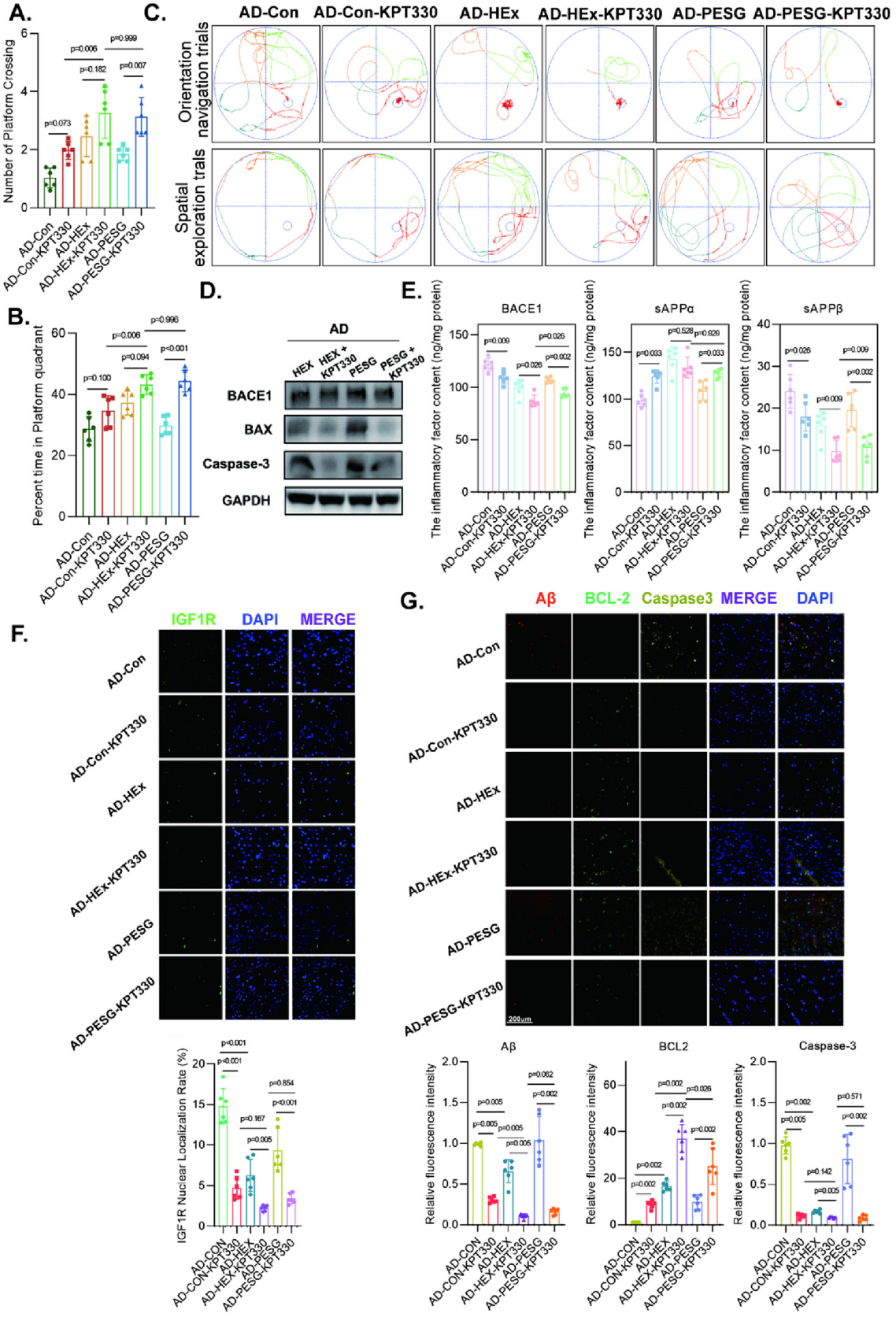
A.
Number of Platform Crossing
p=0.073
p=0.006
p=0.182
p=0.999
p=0.007
AD-Con
AD-Con-KPT330
AD-HEx
AD-HEx-KPT330
AD-PESG
AD-PESG-KPT330
C.
AD-Con
AD-Con-KPT330
AD-HEx
AD-HEx-KPT330
AD-PESG
AD-PESG-KPT330
Orientation navigation trials
Spatial exploration trals
B.
Percent time in Platform quadrant
p=0.100
p=0.008
p=0.094
p=0.996
p<0.001
D.
AD
HEX
HEX + KPT330
PESG
PESG + KPT330
BACE1
BAX
Caspase-3
GAPDH
E.
BACE1
sAPPα
sAPPβ
The inflammatory factor content (ng/mg protein)
F.
IGF1R
DAPI
MERGE
IGF1R Nuclear Localization Rate (%)
G.
Aβ
BCL-2
Caspase3
MERGE
DAPI
200um
Relative fluorescence intensity

an anti-inflammatory effect by inhibiting the production of pro-inflammatory cytokines via the suppression of NF-κB and p38 signaling activation, positing KPT-330's pharmacological stimulation as a promising therapeutic strategy for sepsis [72]. Another study suggested that the XPO1 (CRM1) inhibitor, KPT-330, can inhibit HIF-1α [73]. Our research indicates that KPT-330 may prevent Alzheimer's disease by inhibiting neuroinflammation and preventing cell apoptosis. This is especially pertinent for individuals where regular physical activity might be challenging due to physical constraints or other health issues. KPT-330's influence on the nuclear pore complex, including RanBP2 and SUMO1, might affect IGF1R SUMOylation and subsequently prevent AD. However, while our observations hint at the potential benefits of KPT-330, it's imperative to note that a comprehensive understanding of KPT-330's efficacy and limitations as a substitute for exercise necessitates further in-depth research. We pose the question of whether exercise can promote health by targeting neurological proteins, such as XPO1, through exercise metabolites. The exploration of the mechanisms of interaction between multi-level functional proteins and technologies combining AI-based drugs or nanomaterials may emerge as a potential hotbed of advancement in this domain [74,75].

Physical exercise, as a potential non-pharmacological intervention for AD, has garnered considerable attention [6,76]. Exercise promotes a favorable milieu by enhancing metabolic conditions crucial to overall health [77]. The crosstalk between the nervous system and energy metabolism-related diseases constitutes a significant mechanism leading to neural damage disorders, including AD and cerebral infarction [78–80]. Regular physical activity can improve glucose utilization, augment mitochondrial function, and increase cerebral blood flow, thereby optimizing energy production and supporting neuronal survival [81–83]. One of the key mechanisms by which exercise exerts its role in AD is by alleviating or recalibrating the aberrant metabolism associated with the disease [15,16,84,85]. Exercise not only fosters optimal brain metabolism but also generates bioactive molecules that support neuronal survival and function [86]. Previous studies have identified the IGF1R as a significant regulator of brain metabolism and energy expenditure, indirectly influencing weight management and obesity [87]. In our study, dietary supplements for the various mouse groups were provided to mitigate the confounding variable of weight loss. Nonetheless, given IGF1R's pivotal role in energy metabolism, we surmise that its SUMOylation plays a crucial role in modulating brain metabolism and energy expenditure, potentially constituting a key mechanism through which it ameliorates AD [88]. Our study suggests that physical activity may regulate brain cell metabolism and pathways associated with inflammation and apoptosis by modulating XPO1 and inhibiting the nuclear translocation of IGF1R, thereby suppressing AD.

Our research employed relevant animal models to examine how exercise attenuates neuroinflammation by inhibiting the SUMOylation of IGF1R. It is critical to recognize that these models may not entirely capture the complexity of AD in humans, and that establishing causality necessitates further study [89–91]. Future research endeavors are poised to utilize more direct manipulations of IGF1R SUMOylation and its nuclear translocation to delve deeper into their roles in diminishing exercise-induced neuroinflammation, such as how exercise might regulate the nuclear translocation of XPO1 to modulate SUMOylation. Furthermore, the precise molecular pathways underlying these effects merit additional exploration. This includes determining whether the impacts we documented are confined to moderate-intensity exercise or if varying intensities and forms of exercise engender analogous outcomes. Another consideration arising from our study is the extent to which these molecular alterations contribute to the observed enhancement in cognitive function and the degree to which these insights can be translated into clinical strategies for the management of AD. Drawing on established research, our study elucidates the neuroprotective capacity of physical exercise in AD, notably via the modulation of IGF1R's nuclear translocation and SUMOylation, the attenuation of neuroinflammation, and the enhancement of neuronal survival. Although our findings provide a foundational comprehension, it is essential to delve further into these biological mechanisms and their implications for AD therapeutics. Our research paves the way for future investigations that may lead to the development of exercise-based therapeutic modalities for AD and innovative treatments that target IGF1R SUMOylation.

Conclusion

Our study highlights the potential of physical exercise and IGF1R SUMOylation modulation as key strategies against Alzheimer's Disease. We've unveiled a novel pathway where exercise offers neuroprotection, notably by regulating IGF1R's nuclear translocation and SUMOylation, and by mitigating neuroinflammation. Additionally, the compound KPT-330 emerges as a potential alternative to exercise, especially for those unable to engage in regular physical activity. While our findings pave the way for innovative therapeutic approaches to Alzheimer's Disease, they also underscore the need for deeper research into these mechanisms.

Funding

This research was further bolstered by the Health Shanghai Initiative Special Fund, emphasizing the amalgamation of medicine and sports to pioneer a novel paradigm for healthful exercise (Pro-

Figure 6. Role of KPT-330 in Neuroprotection and its Potential as an Exercise Surrogate in Alzheimer's Disease. (A) Neuroprotective Effects on Platform Crossings: Scatter plot analysis shows an increase in the number of platform crossings in the Alzheimer's disease (AD) mice treated with KPT-330, indicating improved memory retention. The highest improvement was seen in the AD-HEX + KPT-330 and AD-PESG + KPT-330 groups. (n = 6 per group) (B) Time Spent in Target Quadrant: Bar chart illustrates the time percentage spent in the target quadrant during the Morris Water Maze retention phase. AD mice treated with KPT-330 spent more time in the target quadrant compared to control groups, suggesting enhanced spatial memory. (n = 6 per group) (C) Swim Path Analysis during Morris Water Maze Retention Phase: Trajectory plots of swimming paths show that AD mice treated with KPT-330 (AD-HEX + KPT-330 and AD-PESG + KPT-330) exhibited more focused swimming patterns towards the platform, indicative of improved cognitive function compared to control groups. (D) Impact of KPT-330 on Protein Expression: Western blot analysis reveals that KPT-330 treatment in AD mice is associated with decreased expression of pro-apoptotic proteins (BACE1, BAX and Caspase-3) suggesting neuroprotective effects. (E) ELISA Analysis of Alzheimer's Disease Markers: Bar charts show levels of Alzheimer's disease-associated proteins (BACE1, sAPPα, sAPPβ) in hippocampal homogenates. KPT-330 treatment resulted in a reduction of harmful protein levels (BACE1, sAPPβ) and an increase in sAPPα, which could indicate protective effects against AD pathology. (n = 6 per group) (F) Immunofluorescence of IGF1R Nuclear Translocation: Quantitative histograms of IGF1R nuclear localization show a decrease in nuclear IGF1R in AD mice treated with KPT-330, suggesting the drug's capacity to modulate IGF1R nuclear translocation and potentially its signaling pathways. (n = 6 per group) (G) Analysis of Apoptosis through Immunofluorescence: Bar charts represent the intensity of Caspase-3 staining, with reduced expression in AD mice treated with KPT-330, highlighting its potential to inhibit apoptotic processes associated with AD. (n = 6 per group) Statistical significance is denoted by p-values < 0.05, with all data represented as mean ± SD. Detailed statistical results are included in Supplementary Table 1.

ject No. JKSHZX-2022–02). This investigation was underpinned by generous endowments from the National Natural Science Foundation of China (Nos. 8217091186 and 8197090107). Concurrently, financial support was extended by the Natural Science Foundation of Shandong Province (ZR2022MH124), the Youth Science Foundation of Shandong First Medical University (202201–105), the Shandong Medical and Health Technology Development Fund (202103070325), and the Shandong Province Traditional Chinese Medicine Science and Technology Initiative (M−2022216). The endeavor was also championed by Hainan Province Medical and Health Research (19A200123) .

Acknowledgments

We extend our gratitude to the anonymous reviewers whose contributions were pivotal to the successful publication of this study. Our thanks are also due to BioRender (www.biorender.com) for their illustration services provided under Agreement number: AV26DR469X.

Appendix A. Supplementary data

Supplementary data to this article can be found online at https://doi.org/10.1016/j.jare.2024.03.025.

References

[1] Reitz C, Mayeux R. Alzheimer disease: epidemiology, diagnostic criteria, risk factors and biomarkers. Biochem Pharmacol 2014;88:640–51. doi: https://doi.org/10.1016/j.bcp.2013.12.024.
[2] Long JM, Holtzman DM. Alzheimer disease: an update on pathobiology and treatment strategies. Cell 2019;179:312–39. doi: https://doi.org/10.1016/j.cell.2019.09.001.
[3] Bamberger ME, Landreth GE. Inflammation, apoptosis, and alzheimer's disease. Neuroscientist 2002;8:276–83. doi: https://doi.org/10.1177/1073858402008003013.
[4] Sharma P, Srivastava P, Seth A, Tripathi PN, Banerjee AG, Shrivastava SK. Comprehensive review of mechanisms of pathogenesis involved in Alzheimer's disease and potential therapeutic strategies. Prog Neurobiol 2019;174:53–89. doi: https://doi.org/10.1016/j.pneurobio.2018.12.006.
[5] Doine MQ, Martelli A, Hunger MS. Practice of physical exercises as a non-pharmacological strategy in the treatment of alzheimer's disease treatment. S F J of Health 2020;1(41–53). doi: https://doi.org/10.46981/sfjhv1n3-002.
[6] Ribarič S. Physical exercise, a potential non-pharmacological intervention for attenuating neuroinflammation and cognitive decline in alzheimer's disease patients. IJMS 2022;23:3245. doi: https://doi.org/10.3390/ijms23063245.
[7] Bherer L, Erickson KI, Liu-Ambrose T. A review of the effects of physical activity and exercise on cognitive and brain functions in older adults. Journal of Aging Research 2013;2013:1–8. doi: https://doi.org/10.1155/2013/657508.
[8] Gomez-Pinilla F, Hillman C. The Influence of Exercise on Cognitive Abilities. In: Terjung R, editor. Comprehensive Physiology. Wiley; 2013. p. 403–28. doi: https://doi.org/10.1002/cphy.c110063.
[9] Kennedy G, Hardman RJ, Macpherson H, Scholey AB, Pipingas A. How does exercise reduce the rate of age-associated cognitive decline? A Review of Potential Mechanisms JAD 2016;55:1–18. doi: https://doi.org/10.3233/JAD-160665.
[10] Khan MB, Alam H, Siddiqui S, Shaikh MF, Sharma A, Rehman A, et al. Exercise improves cerebral blood flow and functional outcomes in an experimental mouse model of vascular cognitive impairment and dementia (VCID). Transl Stroke Res 2023. doi: https://doi.org/10.1007/s12975-023-01124-w.
[11] Hötting K, Röder B. Beneficial effects of physical exercise on neuroplasticity and cognition. Neurosci Biobehav Rev 2013;37:2243–57. doi: https://doi.org/10.1016/j.neubiorev.2013.04.005.
[12] Lau Y-S, Patki G, Das-Panja K, Le W-D, Ahmad SO. Neuroprotective effects and mechanisms of exercise in a chronic mouse model of parkinson's disease with moderate neurodegeneration: exercise neuroprotection in chronic parkinsonism. Eur J Neurosci 2011;33:1264–74. doi: https://doi.org/10.1111/j.1460-9568.2011.07626.x.
[13] Zhang X, He Q, Huang T, Zhao N, Liang F, Xu B, et al. Treadmill exercise decreases Aβ deposition and counteracts cognitive decline in APP/PS1 mice, possibly via hippocampal microglia modifications. Front Aging Neurosci 2019;11:78. doi: https://doi.org/10.3389/fnagi.2019.00078.
[14] Meng Q, Lin M-S, Tzeng I-S. Relationship between exercise and alzheimer's disease: a narrative literature review. Front Neurosci 2020;14:131. doi: https://doi.org/10.3389/fnins.2020.00131.
[15] Chen Y, Luo Z, Sun Y, Li F, Han Z, Qi B, et al. Exercise improves choroid plexus epithelial cells metabolism to prevent glial cell-associated neurodegeneration. Front Pharmacol 2022;13:1010785. doi: https://doi.org/10.3389/fphar.2022.1010785.
[16] Maliszewska-Cyna E, Lynch M, Oore J, Nagy P, Aubert I. The benefits of exercise and metabolic interventions for the prevention and early treatment of alzheimer's disease. CAR 2016;14:47–60. doi: https://doi.org/10.2174/1567205013666160819125400.
[17] Jang Y, Kwon I, Cosio-Lima L, Wirth C, Vinci DM, Lee Y. Endurance exercise prevents metabolic distress–induced senescence in the hippocampus. Med Sci Sports Exerc 2019;51:2012–24. doi: https://doi.org/10.1249/MSS.0000000000002011.
[18] Zhu Z, Shen J, Zhang Y, Wang J, Sun Y, Liu W, et al. Research Progress in Heart Rate Variability Applications in Exercise Rehabilitation for Cardiovascular Diseases. CVIA 2023;8. 10.15212/CVIA.2023.0071.
[19] Maass A, Düzel S, Brigadski T, Goerke M, Becke A, Sobieray U, et al. Relationships of peripheral IGF-1, VEGF and BDNF levels to exercise-related changes in memory, hippocampal perfusion and volumes in older adults. Neuroimage 2016;131:142–54. doi: https://doi.org/10.1016/j.neuroimage.2015.10.084.
[20] Titus J, Bray NW, Kamkar N, Camicioli R, Nagamatsu LS, Speechley M, et al. The role of physical exercise in modulating peripheral inflammatory and neurotrophic biomarkers in older adults: a systematic review and meta-analysis. Mech Ageing Dev 2021;194:. doi: https://doi.org/10.1016/j.mad.2021.111431111431.
[21] Cardoso S, López I, Piñeiro-Hermida S, Pichel J, Moreira P. IGF1R Deficiency modulates brain signaling pathways and disturbs mitochondria and redox homeostasis. Biomedicines 2021;9:158. doi: https://doi.org/10.3390/biomedicines9020158.
[22] Baek SH. A novel link between SUMO modification and cancer metastasis. Cell Cycle 2006;5:1492–5. doi: https://doi.org/10.4161/cc.5.14.3008.
[23] Sehat B, Tofigh A, Lin Y, Trocmé E, Liljedahl U, Lagergren J, et al. SUMOylation mediates the nuclear translocation and signaling of the IGF-1 receptor. Sci Signal 2010:3. doi: https://doi.org/10.1126/scisignal.2000628.
[24] Fan L, Zhaohong X, Xiangxue W, Yingying X, Xiao Z, Xiaoyan Z, et al. Melatonin ameliorates the progression of alzheimer's disease by inducing TFEB nuclear translocation, promoting mitophagy, and regulating NLRP3 inflammasome activity. Biomed Res Int 2022;2022:1–13. doi: https://doi.org/10.1155/2022/8099459.
[25] Austad SN, Ballinger S, Buford TW, Carter CS, Smith DL, Darley-Usmar V, et al. Targeting whole body metabolism and mitochondrial bioenergetics in the drug development for Alzheimer's disease. Acta Pharm Sin B 2022;12:511–31. doi: https://doi.org/10.1016/j.apsb.2021.06.014.
[26] Coyne AN, Rothstein JD. Nuclear pore complexes — a doorway to neural injury in neurodegeneration. Nat Rev Neurol 2022;18:348–62. doi: https://doi.org/10.1038/s41582-022-00653-6.
[27] Jiang R, Wang M, Shen X, Huang S, Han J, Li L, et al. SUMO1 modification of IGF-1R combining with SNAI2 inhibited osteogenic differentiation of PDLSCs stimulated by high glucose. Stem Cell Res Ther 2021;12:543. doi: https://doi.org/10.1186/s13287-021-02618-w.
[28] Packham S, Warsito D, Lin Y, Sadi S, Karlsson R, Sehat B, et al. Nuclear translocation of IGF-1R via p150Glued and an importin-β/RanBP2-dependent pathway in cancer cells. Oncogene 2015;34:2227–38. doi: https://doi.org/10.1038/onc.2014.165.
[29] Tatham MH, Kim S, Jaffray E, Song J, Chen Y, Hay RT. Unique binding interactions among Ubc9, SUMO and RanBP2 reveal a mechanism for SUMO paralog selection. Nat Struct Mol Biol 2005;12:67–74. doi: https://doi.org/10.1038/nsmb878.
[30] Werner A, Flotho A, Melchior F. The RanBP2/RanGAP1*SUMO1/Ubc9 complex is a multisubunit SUMO E3 ligase. Mol Cell 2012;46:287–98. doi: https://doi.org/10.1016/j.molcel.2012.02.017.
[31] Miyamoto Y, Yoneda Y, Oka M. Protein transport between the nucleus and cytoplasm. Nuclear Architecture and Dynamics, Elsevier 2018:387–403. doi: https://doi.org/10.1016/B978-0-12-803480-4.00025-9.
[32] Archbold HC, Jackson KL, Arora A, Weskamp K, Tank E-M-H, Li X, et al. TDP43 nuclear export and neurodegeneration in models of amyotrophic lateral sclerosis and frontotemporal dementia. Sci Rep 2018;8:4606. doi: https://doi.org/10.1038/s41598-018-22858-w.
[33] Ederle H, Funk C, Abou-Ajram C, Hutten S, Funk EBE, Kehlenbach RH, et al. Nuclear egress of TDP-43 and FUS occurs independently of exportin-1/CRM1. Sci Rep 2018;8:7084. doi: https://doi.org/10.1038/s41598-018-25007-5.
[34] Chou C-C, Zhang Y, Umoh ME, Vaughan SW, Lorenzini I, Liu F, et al. TDP-43 pathology disrupts nuclear pore complexes and nucleocytoplasmic transport in ALS/FTD. Nat Neurosci 2018;21:228–39. doi: https://doi.org/10.1038/s41593-017-0047-3.
[35] Nie D, Huang K, Yin S, Li Y, Xie S, Ma L, et al. KPT-330 inhibition of chromosome region maintenance 1 is cytotoxic and sensitizes chronic myeloid leukemia to Imatinib. Cell Death Discovery 2018;4:48. doi: https://doi.org/10.1038/s41420-018-0049-2.
[36] Kashyap T, Argueta C, Aboukameel A, Unger TJ, Klebanov B, Mohammad RM, et al. Selinexor, a Selective Inhibitor of Nuclear Export (SINE) compound, acts through NF-κB deactivation and combines with proteasome inhibitors to synergistically induce tumor cell death. Oncotarget 2016;7(78883–95). doi: https://doi.org/10.18632/oncotarget.12428.
[37] Crochiere M, Kashyap T, Kalid O, Shechter S, Klebanov B, Senapedis W, et al. Deciphering mechanisms of drug sensitivity and resistance to selective inhibitor of nuclear export (SINE) compounds. BMC Cancer 2015;15:910. doi: https://doi.org/10.1186/s12885-015-1790-z.

[38] He X, Fu Y, Ma L, Yao Y, Ge S, Yang Z, et al. AAV for gene therapy in ocular diseases: progress and prospects. Research 2023;6(0291). doi: https://doi.org/10.34133/research.0291.
[39] McGee SL, Hargreaves M. Exercise adaptations: molecular mechanisms and potential targets for therapeutic benefit. Nat Rev Endocrinol 2020;16:495–505. doi: https://doi.org/10.1038/s41574-020-0377-1.
[40] Reiserer RS, Harrison FE, Syverud DC, McDonald MP. Impaired spatial learning in the APPSwe + PSEN1DeltaE9 bigenic mouse model of Alzheimer's disease. Genes Brain Behav 2007;6:54–65. doi: https://doi.org/10.1111/j.1601-183X.2006.00221.x.
[41] Jankowsky JL, Fadale DJ, Anderson J, Xu GM, Gonzales V, Jenkins NA, et al. Mutant presenilins specifically elevate the levels of the 42 residue beta-amyloid peptide in vivo: evidence for augmentation of a 42-specific gamma secretase. Hum Mol Genet 2004;13:159–70. doi: https://doi.org/10.1093/hmg/ddh019.
[42] Jankowsky JL, Slunt HH, Ratovitski T, Jenkins NA, Copeland NG, Borchelt DR. Co-expression of multiple transgenes in mouse CNS: a comparison of strategies. Biomol Eng 2001;17:157–65. doi: https://doi.org/10.1016/s1389-0344(01)00067-3.
[43] Fernando P, Bonen A, Hoffman-Goetz L. Predicting submaximal oxygen consumption during treadmill running in mice. Can J Physiol Pharmacol 1993;71:854–7. doi: https://doi.org/10.1139/y93-128.
[44] Fisher J, Steele J, Smith D. High- and low-load resistance training: interpretation and practical application of current research findings. Sports Med 2017;47:393–400. doi: https://doi.org/10.1007/s40279-016-0602-1.
[45] Yuan S, Yang J, Jian Y, Lei Y, Yao S, Hu Z, et al. Treadmill exercise modulates intestinal microbes and suppresses LPS displacement to alleviate neuroinflammation in the brains of APP/PS1 mice. Nutrients 2022;14:4134. doi: https://doi.org/10.3390/nu14194134.
[46] Yu H, Zhang C, Xia J, Xu B. Treadmill exercise ameliorates adult hippocampal neurogenesis possibly by adjusting the APP proteolytic pathway in APP/PS1 transgenic mice. IJMS 2021;22:9570. doi: https://doi.org/10.3390/ijms22179570.
[47] Liu Y, Hu P-P, Zhai S, Feng W-X, Zhang R, Li Q, et al. Aquaporin 4 deficiency eliminates the beneficial effects of voluntary exercise in a mouse model of Alzheimer's disease. Neural Regen Res 2022;17:2079. doi: https://doi.org/10.4103/1673-5374.335169.
[48] Taliaferro-Smith L, Oberlick E, Liu T, McGlothen T, Alcaide T, Tobin R, et al. FAK activation is required for IGF1R-mediated regulation of EMT, migration, and invasion in mesenchymal triple negative breast cancer cells. Oncotarget 2015;6(4757–72). doi: https://doi.org/10.18632/oncotarget.3023.
[49] Alehossein P, Taheri M, Tayefeh Ghahremani P, Dakhlallah D, Brown CM, Ishrat T, et al. Transplantation of exercise-induced extracellular vesicles as a promising therapeutic approach in ischemic stroke. Transl Stroke Res 2023;14:211–37. doi: https://doi.org/10.1007/s12975-022-01025-4.
[50] Liang J, Wang H, Zeng Y, Qu Y, Liu Q, Zhao F, et al. Physical exercise promotes brain remodeling by regulating epigenetics, neuroplasticity and neurotrophins. Rev Neurosci 2021;32:615–29. doi: https://doi.org/10.1515/revneuro-2020-0099.
[51] Wyss-Coray T, Rogers J. Inflammation in alzheimer disease–a brief review of the basic science and clinical literature. Cold Spring Harb Perspect Med 2012;2:a006346–a. doi: https://doi.org/10.1101/cshperspect.a006346.
[52] Liu S, Wang S, Gu R, Che N, Wang J, Cheng J, et al. The XPO1 inhibitor KPT-8602 ameliorates parkinson's disease by inhibiting the NF-κB/NLRP3 pathway. Front Pharmacol 2022;13:. doi: https://doi.org/10.3389/fphar.2022.847605847605.
[53] Halliday G, Robinson SR, Shepherd C, Kril J. Alzheimer's disease and inflammation: a review of cellular and therapeutic mechanisms. Clin Exp Pharmacol Physiol 2000;27:1–8. doi: https://doi.org/10.1046/j.1440-1681.2000.03200.x.
[54] Ahmadi F, Khalatbary A. A review on the neuroprotective effects of hyperbaric oxygen therapy. Med Gas Res 2021;11:72. doi: https://doi.org/10.4103/2045-9912.311498.
[55] Wu X, Liang T-Y, Wang Z, Chen G. The role of hyperbaric oxygen therapy in inflammatory bowel disease: a narrative review. Med Gas Res 2021;11:66. doi: https://doi.org/10.4103/2045-9912.311497.
[56] Lu Y, Dong Y, Tucker D, Wang R, Ahmed ME, Brann D, et al. Treadmill exercise exerts neuroprotection and regulates microglial polarization and oxidative stress in a streptozotocin-induced rat model of sporadic alzheimer's disease. JAD 2017;56:1469–84. doi: https://doi.org/10.3233/JAD-160869.
[57] Nichol KE, Poon WW, Parachikova AI, Cribbs DH, Glabe CG, Cotman CW. Exercise alters the immune profile in Tg2576 Alzheimer mice toward a response coincident with improved cognitive performance and decreased amyloid. J Neuroinflammation 2008;5:13. doi: https://doi.org/10.1186/1742-2094-5-13.
[58] Li Z, Chen Q, Liu J, Du Y. Physical exercise ameliorates the cognitive function and attenuates the neuroinflammation of alzheimer's disease via miR-129–5p. Dement Geriatr Cogn Disord 2020;49:163–9. doi: https://doi.org/10.1159/000507285.
[59] Preeti K, Sood A, Fernandes V. Metabolic regulation of glia and their neuroinflammatory role in alzheimer's disease. Cell Mol Neurobiol 2022;42:2527–51. doi: https://doi.org/10.1007/s10571-021-01147-7.
[60] Huang D-X, Yu X, Yu W-J, Zhang X-M, Liu C, Liu H-P, et al. Calcium signaling regulated by cellular membrane systems and calcium homeostasis perturbed in alzheimer's disease. Front Cell Dev Biol 2022;10:. doi: https://doi.org/10.3389/fcell.2022.834962834962.
[61] Specht H, Slavov N. Beyond protein sequence: protein isomerization in alzheimer's disease. J Proteome Res 2022;21:299–300. doi: https://doi.org/10.1021/acs.jproteome.2c00016.
[62] Martin L, Latypova X, Terro F. Post-translational modifications of tau protein: implications for Alzheimer's disease. Neurochem Int 2011;58:458–71. doi: https://doi.org/10.1016/j.neuint.2010.12.023.
[63] Xu W, Fang F, Ding J, Wu C. Dysregulation of Rab5-mediated endocytic pathways in Alzheimer's disease. Traffic 2018;19:253–62. doi: https://doi.org/10.1111/tra.12547.
[64] Benarroch EE. Nucleocytoplasmic transport: Mechanisms and involvement in neurodegenerative disease. Neurology 2019;92:757–64. doi: https://doi.org/10.1212/WNL.0000000000007305.
[65] Jimenez L, Mayoral-Varo V, Amenábar C, Ortega J, Sequeira JGN, Machuqueiro M, et al. Multiplexed cellular profiling identifies an organoselenium compound as an inhibitor of CRM1 -mediated nuclear export. Traffic 2022;23:587–99. doi: https://doi.org/10.1111/tra.12872.
[66] Luo G, Wang X, Liu C. MiR-483-3p improves learning and memory abilities via XPO1 in Alzheimer's disease. Brain and Behavior 2022;12:e2680.
[67] Koyama M, Matsuura Y. Mechanistic insights from the recent structures of the CRM1 nuclear export complex and its disassembly intermediate. Biophysics 2012;8:145–50. doi: https://doi.org/10.2142/biophysics.8.145.
[68] Chughtai S. The nuclear translocation of insulin-like growth factor receptor and its significance in cancer cell survival. Cell Biochem Funct 2020;38:347–51. doi: https://doi.org/10.1002/cbf.3479.
[69] Ritterhoff T, Das H, Hofhaus G, Schröder RR, Flotho A, Melchior F. The RanBP2/RanGAP1*SUMO1/Ubc9 SUMO E3 ligase is a disassembly machine for Crm1-dependent nuclear export complexes. Nat Commun 2016;7:11482. doi: https://doi.org/10.1038/ncomms11482.
[70] Seeler J-S, Dejean A. Nuclear and unclear functions of SUMO. Nat Rev Mol Cell Biol 2003;4:690–9. doi: https://doi.org/10.1038/nrm1200.
[71] Santiago A, Li D, Zhao LY, Godsey A, Liao D. p53 SUMOylation promotes its nuclear export by facilitating its release from the nuclear export receptor CRM1. MBoC 2013;24:2739–52. doi: https://doi.org/10.1091/mbc.e12-10-0771.
[72] Wu M, Gui H, Feng Z, Xu H, Li G, Li M, et al. KPT-330, a potent and selective CRM1 inhibitor, exhibits anti-inflammation effects and protection against sepsis. Biochem Biophys Res Commun 2018;503:1773–9. doi: https://doi.org/10.1016/j.bbrc.2018.07.112.
[73] Von Fallois M, Kosyna FK, Mandl M, Landesman Y, Dunst J, Depping R. Selinexor decreases HIF-1α via inhibition of CRM1 in human osteosarcoma and hepatoma cells associated with an increased radiosensitivity. J Cancer Res Clin Oncol 2021;147:2025–33. doi: https://doi.org/10.1007/s00432-021-03626-2.
[74] Yang Y, Wang J. Exploring the multi-level interaction mechanism between drugs and targets based on artificial intelligence. CI 2022;13. doi: https://doi.org/10.58567/ci01020004.
[75] Yang H, Li C, Xie Q. Advances in the use of nanomaterials in tumour therapy. Challenges and Prospects CI 2023;2(37–48). doi: https://doi.org/10.58567/ci02020004.
[76] Chen Y, Sun Y, Luo Z, Chen X, Wang Y, Qi B, et al. Exercise modifies the transcriptional regulatory features of monocytes in alzheimer's patients: a multi-omics integration analysis based on single cell technology. Front Aging Neurosci 2022;14:. doi: https://doi.org/10.3389/fnagi.2022.881488881488.
[77] Thyfault JP, Bergouignan A. Exercise and metabolic health: beyond skeletal muscle. Diabetologia 2020;63:1464–74. doi: https://doi.org/10.1007/s00125-020-05177-6.
[78] Jong G-P, Lin T-K, Liao P-L, Huang J-Y, Yang T-Y, Pan L-F. Risk of new-onset stroke in patients with Type 2 diabetes with chronic kidney disease on sodium-glucose Co-transporter-2 inhibitor users. Transl Stroke Res 2023. doi: https://doi.org/10.1007/s12975-023-01174-0.
[79] Bielanin JP, Sun D. Significance of microglial energy metabolism in maintaining brain homeostasis. Transl Stroke Res 2023;14:435–7. doi: https://doi.org/10.1007/s12975-022-01069-6.
[80] Zhang W, Dong XY, Huang R. Gut microbiota in ischemic stroke: role of gut bacteria-derived metabolites. Transl Stroke Res 2023;14:811–28. doi: https://doi.org/10.1007/s12975-022-01096-3.
[81] Seifert T, Secher NH. Sympathetic influence on cerebral blood flow and metabolism during exercise in humans. Prog Neurobiol 2011;95:406–26. doi: https://doi.org/10.1016/j.pneurobio.2011.09.008.
[82] Maugeri G, D'Agata V, Magrì B, Roggio F, Castorina A, Ravalli S, et al. Neuroprotective effects of physical activity via the adaptation of astrocytes. Cells 2021;10:1542. doi: https://doi.org/10.3390/cells10061542.
[83] Chen Y, Sun Y, Luo Z, Lin J, Qi B, Kang X, et al. Potential mechanism underlying exercise upregulated circulating blood exosome miR-215-5p to prevent necroptosis of neuronal cells and a model for early diagnosis of alzheimer's disease. Front Aging Neurosci 2022;14:. doi: https://doi.org/10.3389/fnagi.2022.860364860364.
[84] Ying N, Luo H, Li B, Gong K, Shu Q, Liang F, et al. Exercise alleviates behavioral disorders but shapes brain metabolism of APP/PS1 Mice in a region- and exercise-specific manner. J Proteome Res 2023;22:1649–59. doi: https://doi.org/10.1021/acs.jproteome.2c00691.
[85] Guo X, Gu S, Wang J, Sun H, Zhang Y, Yu P, et al. Protective effect of mesenchymal stem cell-derived exosomal treatment of hippocampal neurons

against oxygen-glucose deprivation/reperfusion-induced injury. World J Emerg Med 2022;13:46. doi: https://doi.org/10.5847/wjem.j.1920-8642.2022.015.
[86] Camandola S, Mattson MP. Brain metabolism in health, aging, and neurodegeneration. EMBO J 2017;36(1474–92).
[87] Cheng CM, Reinhardt RR, Lee W-H, Joncas G, Patel SC, Bondy CA. Insulin-like growth factor 1 regulates developing brain glucose metabolism. Proc Natl Acad Sci USA 2000;97:10236–41. doi: https://doi.org/10.1073/pnas.170008497.
[88] Procaccini C, Santopaolo M, Faicchia D, Colamatteo A, Formisano L, De Candia P, et al. Role of metabolism in neurodegenerative disorders. Metabolism 2016;65:1376–90. doi: https://doi.org/10.1016/j.metabol.2016.05.018.
[89] Webster SJ, Bachstetter AD, Nelson PT, Schmitt FA, Van Eldik LJ. Using mice to model Alzheimer's dementia: an overview of the clinical disease and the preclinical behavioral changes in 10 mouse models. Front Genet 2014;5. doi: https://doi.org/10.3389/fgene.2014.00088.
[90] Cohen RM, Rezai-Zadeh K, Weitz TM, Rentsendorj A, Gate D, Spivak I, et al. A transgenic alzheimer rat with plaques, tau pathology, behavioral impairment, oligomeric Aβ, and frank neuronal loss. J Neurosci 2013;33:6245–56. doi: https://doi.org/10.1523/JNEUROSCI.3672-12.2013.
[91] De Felice FG, Munoz DP. Opportunities and challenges in developing relevant animal models for Alzheimer's disease. Ageing Res Rev 2016;26:112–4. doi: https://doi.org/10.1016/j.arr.2016.01.006.